

12-15-2014

High Level Control Implementation for a Residential Smart Grid Power System

Hang Xu

University of South Carolina - Columbia

Follow this and additional works at: <http://scholarcommons.sc.edu/etd>

Recommended Citation

Xu, H.(2014). *High Level Control Implementation for a Residential Smart Grid Power System*. (Master's thesis). Retrieved from <http://scholarcommons.sc.edu/etd/2953>

This Open Access Thesis is brought to you for free and open access by Scholar Commons. It has been accepted for inclusion in Theses and Dissertations by an authorized administrator of Scholar Commons. For more information, please contact SCHOLARC@mailbox.sc.edu.

HIGH LEVEL CONTROL IMPLEMENTATION FOR A RESIDENTIAL SMART GRID
POWER SYSTEM

by

Hang Xu

Bachelor of Science
Southeast University, 2009

Submitted in Partial Fulfillment of the Requirements

For the Degree of Master of Science in

Electrical Engineering

College of Engineering and Computing

University of South Carolina

2014

Accepted by:

Roger Dougal, Director of Thesis

Xiaofeng Wang, Reader

Lacy Ford, Vice Provost and Dean of Graduate Studies

© Copyright by Hang Xu, 2014
All Rights Reserved.

DEDICATION

This thesis is dedicated to my family, who has supported me in my study life so far, both emotionally and financially. And this thesis is also dedicated to all my instructors along my study life, who have instilled their wisdom essentials into my future life.

ACKNOWLEDGEMENTS

I would like to thank my advisor, Dr. Roger Dougal, who gave me a great project for my master degree research and my other advisor: Dr. Xiaofeng Wang, both of whom have supported me with their knowledge, experience, and advice. Thank you to the rest of my teachers at USC, most notably the power group: Dr. Enrico Santi, Dr. Charles Brice, and Dr. Herbert Ginn. Thank you most of all to Rich Smart, Robert Motte, Tyler Price, Pietro Cairoli, Cale Workman, and all of my colleagues in the electrical engineering department, whose love, friendship, and support I could not have accomplished this without.

I would also like to acknowledge the GRAPES IAB for their data, industry insight, and funding.

ABSTRACT

With the environment protection and energy usage efficiency promotion issues concerned more and more by governments and industries these days, smart grid technologies have been in rapid development. On this new technology stage, residential site power management system has become a star. This paper introduces the concept, development of two high level control methods for “Smart Green Power Node” (SGPN), solutions of demand side energy management system.

One control algorithm is optimal model method which uses the predictive data of a battery model with electrical parameters and pricing methods, to keep scheduling the optimal control input on the receding time horizon continuously. The other one is rule-based method which determines each time instant’s control inputs by logical judgment upon current and past battery electrical parameters and price states without model and predictive data in an easier implementing and faster calculating manner. Both algorithm systems incorporate necessary data such as photovoltaic solar power generation, user input, hardware states and load power information, as well as a TOU pricing schedule as inputs to the novel system control algorithm to achieve money saving for both electricity supplier and homeowner. Compared to commercial energy management systems which exist, this system can effectively eliminate the need for human interaction and intelligently regulate house power flow without complicated inputs from homeowner except some basic preferences.

According to the simulation of SGPN models comparison results carried out in MATLAB environment, the rule-based method can provide an annual total credit earn of more than \$1000, based on reasonable industrial electric price and residential side feed-in tariff, yet guarantee a micro-second level calculation rate, which is valuable for real-time use scenario. And the load management during peak time is able to limit the average grid power to utility acceptable level. Moreover, the standalone mode DC bus voltage maintenance capability empowers the system's self-sufficiency during grid outage period. On the other hand, the optimal model method is highly dependent on the accurate predictive model, which could not be practically economically efficient at present to implement but shows the optimality than rule-based method in theory and the potential of guarantee more residential profit in practice if such accurate model can be derived. These results show SGPN's potential market value for both electricity consumers and providers.

TABLE OF CONTENTS

DEDICATION	iii
ACKNOWLEDGEMENTS.....	iv
ABSTRACT	v
LIST OF FIGURES	ix
CHAPTER1: INTRODUCTION	1
CHAPTER 2: SYSTEM TOPOLOGY	5
2.1 SGPN TOPOLOGY	5
2.2 HIGH LEVEL CONTROL OUTPUTS AND INPUTS.....	5
2.3 HIGH LEVEL CONTROL MODES	8
CHAPTER 3: HIGH LEVEL CONTROL DETAIL.....	11
3.1 PRICING INFORMATION	11
3.2 WEATHER INFORMATION	13
3.3 BATTERY SYSTEM.....	15
3.4 CORE CONTROL ALGORITHM STRUCTURE	26
3.6 LOAD SWITCHES PRIORITY CONTROL	44
3.7 THERMAL LOAD CONTROL.....	46
3.8 POWER FLOW BALANCE CONTROL	52
3.9 RULE-BASED ALGORITHM CODE.....	57
CHAPTER 4: SYSTEM SIMULATION & RESULTS.....	75

4.1 SIMULATION DIAGRAM	75
4.2 SIMULATION PARAMETERS	77
4.3 SIMULATION RESULTS	77
4.4 RESULTS ANALYSIS	81
4.5 CONCLUSION	86
REFERENCES	87
APPENDIX A: SGPN HARDWARE STRUCTURE	90
A.1 SUBSYSTEM COMPONENTS	90
A.2 INTERMEDIATE CONNECTION COMPONENTS	91
A.3 HIGH LEVEL AND LOW LEVEL CONTROL HIERARCHY	94

LIST OF FIGURES

Figure 2.1 SGPN System Control Modules	6
Figure 2.2 SGPN outputs and inputs.....	7
Figure 2.3 SGPN three operation modes	9
Figure 3.1 Effect of DOD and cycle number per year on wet battery at 25°C [13]	25
Figure 3.2 Battery use current region within constraints for optimal control method.....	26
Figure 3.3 Top structure of SGPN algorithm in three modes	26
Figure 3.4 Battery use all subcases corresponding to price	33
Figure 3.5 Comparison between sigmoid and sgn functions	34
Figure 3.6 Battery use cost rate when solar power larger than load power	37
Figure 3.7 Battery use cost rate when solar power less than load power	38
Figure 3.8 Battery aging cost rate when discharging.....	38
Figure 3.9 Rule-based algorithm for battery use in automatic response mode.....	43
Figure 3.10 Load switches priority control algorithm flow chart.....	46
Figure 3.11 HV air-condition working principle diagram [25]	47
Figure 3.12 HVAC Simulink model with both heating and cooling functions	50
Figure 3.13 Room temperature curve under cooling mode	51
Figure 3.14 HVAC power curve under cooling mode	51
Figure 3.15 Power flow balance control algorithm flow chart for standalone mode	54
Figure 4.1 SGPN Simulink block diagram	76
Figure 4.2 Simulation parameters	77

Figure 4.3 Electric price and FIT profiles for optimal model method.....	78
Figure 4.4 Battery current & voltage, solar & load power and daily accumulated cost in optimal model method	79
Figure 4.5 Electric price and FIT profiles for rule-based algorithm.....	80
Figure 4.6 Battery current & voltage, solar & load power and daily accumulated cost in general rule-based algorithm.....	80
Figure 4.7 Battery current & voltage, solar & load power and daily accumulated cost in enhanced rule-based algorithm	81
Figure 4.8 Load curtailment mode battery current & voltage, solar power & grid power	83
Figure 4.9 Load curtailment mode uncontrolled, controlled load profiles	83
Figure 4.10 Standalone mode battery current & voltage, solar power & load power, DC bus voltage plot.....	85
Figure A.1 SGPN Control 5-layer Hierarchy Architecture	94

CHAPTER1

INTRODUCTION

Utilizing renewable energy sources is essential issue for human future. As the development of human civilization, we tend to rely on electrical and electronic systems and technologies more and more to deal with tasks which are either impossible or inefficient for human labor. And presently, most of the power supply sources for these systems are dependent on traditional fossil energy sources, like coal, oil and gas. The reason for the irreplaceability of such energy sources is the lowest cost such as source gathering, energy extraction and responding human management cost against energy generation output among all sources list. However, there are many problems related to these fossil fuels. One is the earth's total amount and the local distribution of these fuels is unmatched to the rapid development speed of our world [1]. Another problem is the green house gases emission using these fossil sources during electric generation process have been threatening our environment by global warming effect. As a result, new sorts of renewable energy sources, such as solar energy, wind energy and hydroelectric energy are highly welcomed to gradually reduce and replace the portion of fossil fuels for our sustainable civilization in the future.

Besides, increasing electrical energy usage efficiency is always desired on two primary aspects. One is from energy generation side, that utilities would like to make their daily energy generation more even, which means they could reduce additional

infrastructures' cost just for supplying load peak. One is from energy consumption side, users would like to regulate their daily electrical usage according to electric billing strategies to achieve cost saving and/or credit earned and also they would like this service can be done automatically with only users preference inputs.

All of these modern energy usage issues are requiring a kind of technology and system, which have the ability to incorporate renewable energy sources and enable the information exchange between energy supply and demand sides to increase electric usage efficiency and make profit. In this background, "Smart Grid" concept is proposed and is being researched in worldwide.

According to the definition from Wikipedia, "smart grid is a modernized electrical grid that uses information and communications technology to gather and act on information, such as information about the behaviors of suppliers and consumers, in an automated fashion to improve the efficiency, reliability, economics, and sustainability of the production and distribution of electricity".[2]

Comparing with the traditional grid, smart grid has several advantageous features. One is smart grid gathers digital control technology to let separated smart decision-making devices available for large number of residential sites. One is smart grid focuses on the real-time information exchange and process from all interacting components, in such way making a real-time optimization control possible. Another feature is smart grid enables much more flexibility for power device network topology. One day, we can combine different power sources, smart grid measurements, smart grid control devices and our usage applications following smart grid standards to construct our own power systems, just like playing building blocks.

Based on smart grid technologies, a number of commercial or near-commercial products aiming at residential use [3][4] have been produced. There are four opportunities seen to further advance the technologies in this field – modularity to support a diverse application landscape, high efficiency to reduce energy losses, an ability to operate in standalone mode to support islanding during grid outages or off-grid uses, and a high level of intelligent automation to minimize user input.

These capabilities have been built into an energy management system that is referred to as the Smart Green Power Node (SGPN). In comparison to the automated energy management system presented in [4], which uses Dynamic Programming (DP) optimization, SGPN takes convex optimization or rule-based method, which avoids the phenomenon called “Curse of Dimension”, when the optimization stages are large enough in DP algorithm. With the approach taken by SGPN, it has the ability to implement a more balanced system between calculation rate and accuracy in an efficient and economic manner. Also, the SGPN has the ability to detect when grid power is unavailable, safely disconnect using proper islanding techniques [5], and then act as an independent supplier maintaining power to the home.

The following sections will follow this sequence to introduce the SGPN high level control system. In Chapter 2, the topology of the whole software and hardware system is presented to show the relationship between high level (software) part and low level (hardware) part and all the SGPN working modes will also be presented. In Chapter 3, high level control core algorithms will be presented step by step. Two sorts of algorithms, optimal model method and general rule-based (GRB)/enhanced rule-based (ERB) algorithms, will be expanded. In Chapter 4, simulation and results for high level control

system will be presented and these simulations are done in Matlab platform Simulink environment.

CHAPTER 2

SYSTEM TOPOLOGY

2.1 SGPN TOPOLOGY

This chapter introduces SGPN's entire structure, which includes subsystems connection topology, high level control outputs & inputs and high level control modes.

We start in a big picture first as shown in Figure 2.1. Here the block diagram of SGPN is shown and we can find there are several important low level terminal subsystems in this topology: on-site energy source (PV panel), off-site energy source (grid), energy storage subsystem and load group. There are also intermediate blocks between hardware terminals, which are converters or switches. Since this paper addresses on the high level control part of SGPN system, I will not go deeply into each hardware subsystem but put the hardware information into Appendix A. The high level part will be introduced from the outputs and inputs interaction with surrounding subsystems first, then three operation modes for high level control.

2.2 HIGH LEVEL CONTROL OUTPUTS AND INPUTS

Here we focus on the high level control part and to have a deeper insight of high level control, we first have a look at the high level control inputs and outputs shown in Figure 2.2.

There are three control targets (control outputs) in high level control system: battery use current reference, PV panel's power reference and load group switches

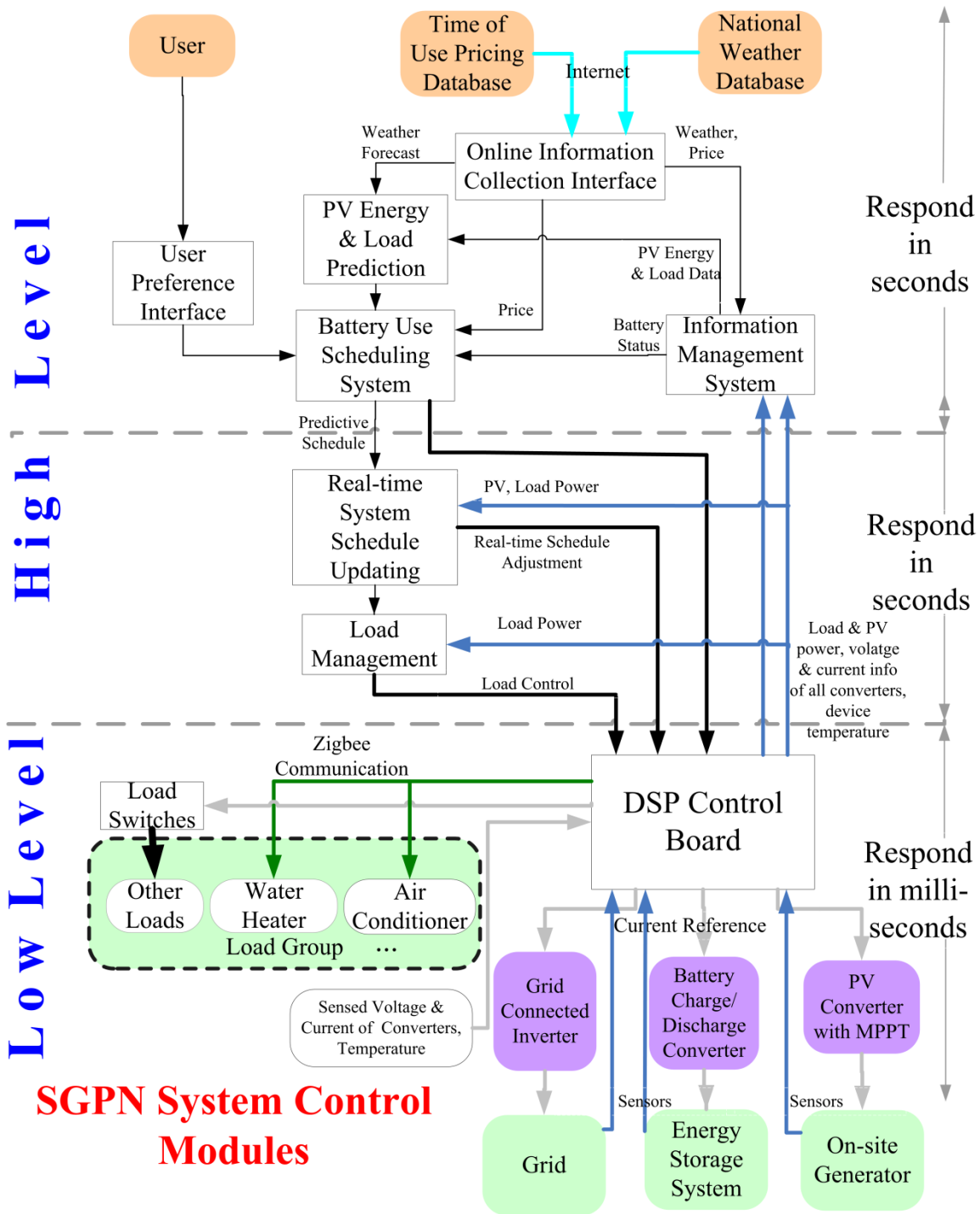


Figure 2.1 SGPN System Control Modules

(and/or thermal load set point). Battery current reference is used to control battery power and the reason of this choice is that battery is the only continuously power adjustable

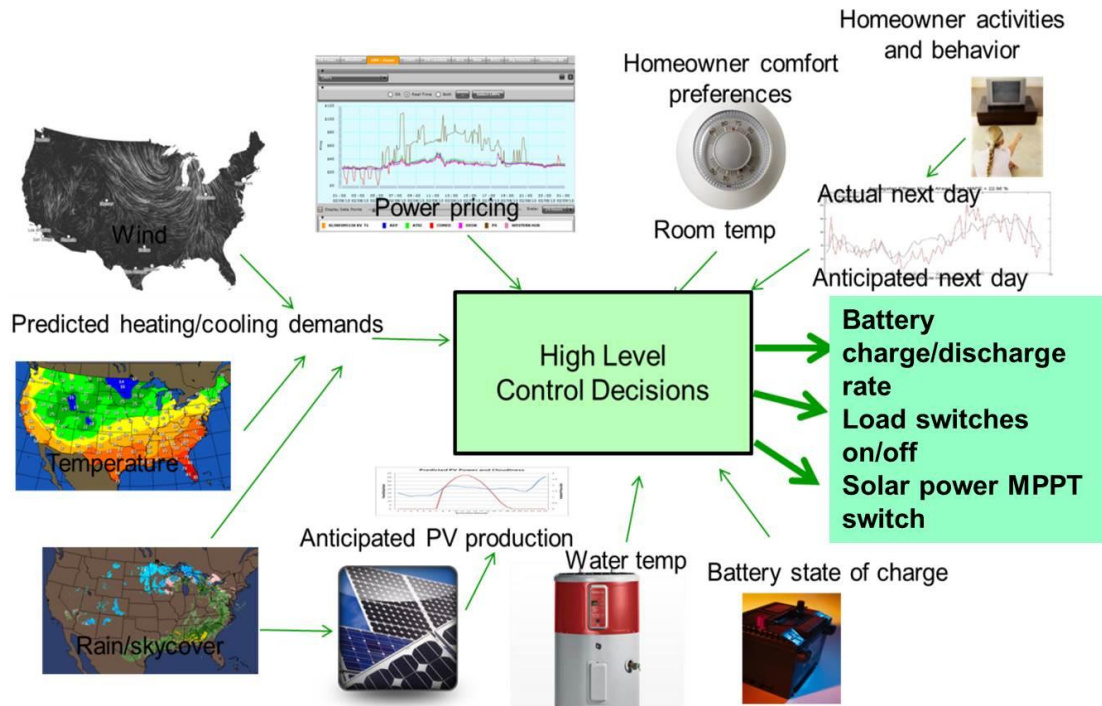


Figure 2.2 SGPN outputs and inputs

variable in the system's normal operation conditions comparing with all other power generating and consuming units: PV panel (normally in maximum power point tracking (MPPT) mode not adjustable), loads (can primarily be discretely switched on and off) and grid (balances the total house electric usage when it is connected to SGPN, and stops power supply when disconnected). PV panel's maximum power point track is always turned on to use solar power as much as possible, except for in standalone mode, where MPPT may be turned off if solar power is surplus to the total present load and battery charging accommodation. The load group switches control is available only in load curtailment mode and standalone mode, and is carried out after comparing the load priority of presently working high power loads. Besides, thermal load set point control is a complementary for load switch control, since home use thermal loads such as HVAC and water heater consume over 50% of total home electric usage [6]. So taking care of

these loads has much scope to save money for homeowners.

To calculate and determine the high level control outputs, the system uses core algorithm with inputs of electric price, weather condition, battery states, thermal load states, load profiles and user preferences. All these inputs will be extended in chapter 3 in detail.

2.3 HIGH LEVEL CONTROL MODES

High level control outputs and inputs part shows how high level control interacts with peripheral subsystems or terminals. And the internal structure of high level control is now shown here.

Our SGPN high level control has three high level modes: automatic response mode, load curtailment mode and standalone mode as shown in Figure 2.3. Automatic response mode is assumed to be the regular operating mode of the system, in which it automatically responds to electric price, present and/or anticipated solar power and loads power to determine the battery use schedule. The detail of the scheduling algorithm will be discussed in chapter 3 with a comparison between optima model method and rule-based method. Another task during automatic response mode is to control thermal loads according to homeowner's preference. SGPN system would not force the change of thermal set point, but instead provide the suggestion about how to change set point to save cost and then record and retrieve homeowner's preference automatically later. And automatic response mode is active when there is neither a grid-off signal from grid sensor nor load curtailment operation being executed.

Load curtailment mode is started only when a request is issued by the utility or an aggregator (a negotiator between utility and SGPN about curtailment and reward) and is

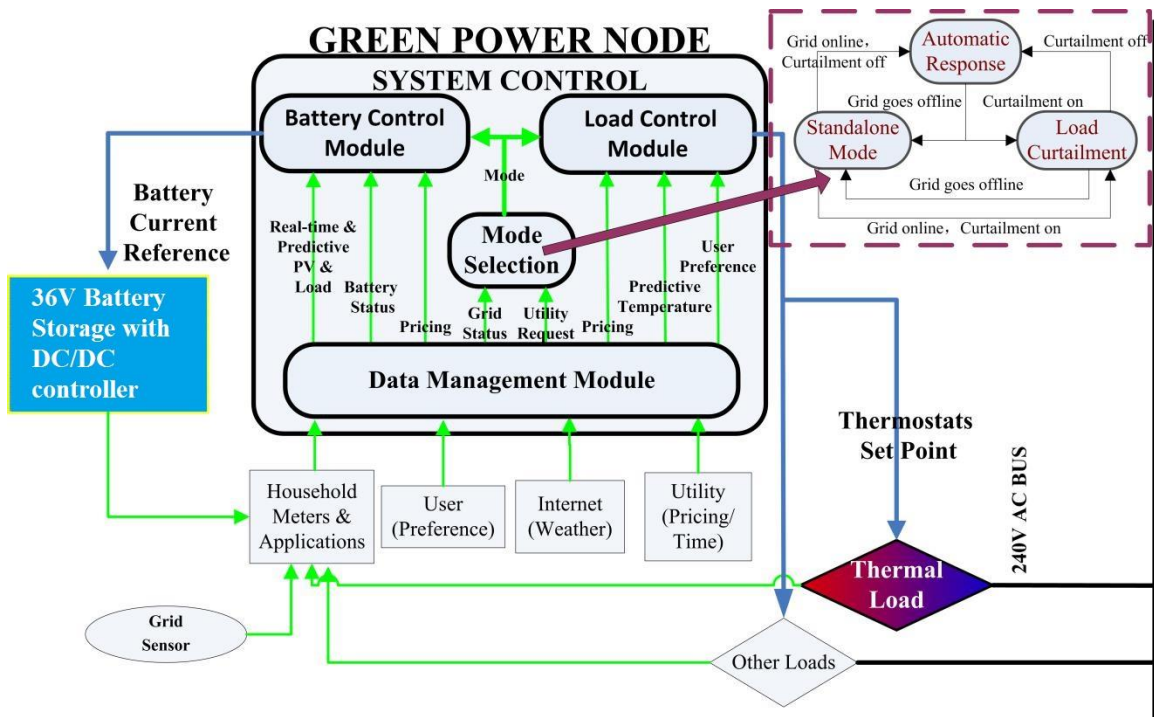


Figure 2.3 SGPN three operation modes

acknowledged by SGPN itself or through SGPN by user reference. The request sending and acknowledgement can be ahead of the curtailment execution period. And there are different kinds of curtailment requests. In one case, a grid power limit is determined based on electric generation conditions of utility or determined by the aggregator's power use limit assignment algorithm. The homeowner agrees and actually succeeds to keep grid demand below this limit during a specified period can get a reward according to utility or aggregator rewarding policy. In another case, utility may directly transform the curtailment request into a real-time fluctuating electric pricing, which will be introduced in chapter 3.1 pricing section. Load curtailment is realized by both load switches group control and the thermal load control, which will be extended in chapter 3.5.

The standalone mode is started only when the grid states sensors inform SGPN

system grid power has gone down. This refers to an emergency of grid energy shortage period, which could be from seconds to days. During this grid outage, SGPN can supply uninterrupted power to the house from battery and/or on-site generators. The stored energy in the battery determines the length home loads can be maintained. During off-site energy outage, lower priority loads will be automatically turned off by load switches group control and electric usage and generation are closely monitored to maintain a balanced on-site grid.

CHAPTER 3

HIGH LEVEL CONTROL DETAIL

3.1 PRICING INFORMATION

3.1.1 ELECTRICITY PRICING

Presently the most widely used pricing method for residential regulatory framework is Time of Use (TOU), either two-tier or three-tier structure. Besides, another pricing structure Real Time Pricing (RTP) has been proposed and researched to show its potential advantages for future smart grid application [7].

Basically, electric price shows how much the cost utilities would take to serve customers electric usage. Traditionally, utility use constant price as an average value of their energy generation cost daily, monthly or annually. As a result, consumer has the right to demand any amount of electricity and pays a constant and infrequently updated price, which accustoms consumer the unawareness of planning and conserving energy use. So a demand-sensitive time varying pricing structure is desired and it has been proven a strategy that allows more service within capacity constraints of the current utility service system infrastructure by many service industries. [4] The TOU structure is the simplest improved form as time varying pricing, which is in some extent still a constant average price value during certain period. And we can expect real-time pricing, which shows the time varying real-time and predictive electricity generation cost of utilities, would be more and more widely used in smart grid technologies such as SGPN in our future lives.

Although there are primarily two different pricing methods, SGPN has the ability to deal with both cases and therefore provide a generic enough approach to work in a variety of regions and policies. Since TOU can be treated as a special case of RTP, in our system, only RTP structure will be used for optimal model method and rule-based algorithm simulations. And the different requirement of price data between these two algorithms lies in that, for optimal model method, system requires both real-time and predictive price data, however, for rule-based algorithm, predictive price data are not necessary.

Instead of predicting the time varying price by itself in optimal model method, SGPN retrieves real-time and predictive price through internet communication of information management subsystem to make cost saving and load peak shaving decisions. Because utility itself owns more convenience to record and analyze historic and real-time data using statistics method, it is much more powerful to get an accurate prediction result than individual SGPN system. Based on this reason, SGPN would retrieve price data instead of predicting by itself. In the present prototype model implementation, we use synthesized RTP method in reasonable style which will be shown in Chapter 4.

3.1.2 PV FEED-IN TARIFF

The policies that govern the premium price of photovoltaic energy fed into the grid are enforced at the state level to incentivize solar panels and have been used throughout the world. However, the detail pricing policies for such feed-in solar energy are distinct nationally and regionally. For example, Germany is the world leader in solar energy generation, partly because of a high feed-in tariff (FIT), currently about 48.89 cents/kWh. Many US states have begun using high feed-in tariffs, particularly California

and Hawaii. Many states, such as South Carolina, have no feed-in tariffs. As such, solar energy in these states is bought by utilities at “avoided cost”. In other words, they only pay the cost they avoided by not buying traditional generation using the cheapest fuel [8].

For a general case, FIT follows the principle of higher premium price during peak time so for an initial simple implementation, in the simulation, we use synthesized FIT rate which is a little higher than RTP during most of daily time. By present policy, FIT only pays for the energy fed into the grid when solar power exceeds the home load and means nothing for using battery energy to feed into the grid. And this is easy to understand that FIT is designed to encourage the usage of renewable energy and a system without any renewable energy source can also feed into the system with the help of energy storage devices. However, this does not mean we would not use battery power to reduce grid burden and thus the electric cost when power price goes high in the present policy frame. Moreover, in future application, this policy may be changed to fully satisfy residential power purchase/sale marketing requirement, which does not tell the difference between residential power sources. So in the long run, in this version control algorithm, battery can be discharged to feed grid directly.

3.2 WEATHER INFORMATION

The weather information significant for SGPN decision is cloudiness, ambient temperature, windiness and humidity. And each kind of information has effect on either solar power input or HVAC thermal load control.

All these four sorts of information can be used for solar power prediction for optimal model method and they are required to retrieve from weather forecast department via internet instead of predicting them by SGPN itself. Because there are randomly

varying and difficultly predictable weather factors for individual SGPN, it would be a more efficient architecture to centralize this service on weather forecast department's much more powerful prediction ability, which refers to much huger volume of weather data and much more advanced calculation hardware and software than separately distributed SGPN systems. Then distributed SGPN would access accurate enough data from this center.

Based on these inputs, insolation power could be predicted through clear sky radiation model along with local field parameters adaptive learning through artificial neural network algorithm [9]. The cloudiness also influences solar power input significantly. However to accurately predict the cloudiness effect specifically for each SGPN's PV panel site, would be difficult by just using weather forecast information, since either the forecast does not provide SGPN interpretable weather info presently or there are other factors like surrounding building shading to greatly interfere solar power prediction. So the neural network algorithm is a good attempt to predict specific solar power at each site.

Besides PV power prediction, weather information is used as thermal parameters in HVAC thermal load control. The insolation on the surface of a house and the average ambient temperature over house are the two main factors to influence the internal thermal state of a house. Although windiness and humidity also have effect on house internal thermal state, however, generally assuming in a window-closed house for air conditioning use, they primarily make effect indirectly by air heat conduction, and evaporation acceleration through the house surface/wall, which inherently contribute to the real-time house surface temperature measured by thermal sensors on the surfaces [10].

3.3 BATTERY SYSTEM

Based on NREL's investigation, lead-acid battery, which has relatively low maintenance requirements and costs, has been used for residential solar electric systems for a long time and is still the best choice for this application [11]. So we need to have further insight into the electrical parameters and structure of lead-acid battery in order to implement control and also prolong the cycle life of battery system. Here for a general battery, SGPN utilizes the parameters from battery specification, but in the future as the technology of smart battery becomes mature, we can expect there would be embedded parameter monitoring system and compatible interface toward smart grid management systems internally built in battery system.

There are several essential electrical parameters or concerns of battery system and here they are clarified.

3.3.1 BATTERY CAPACITY

Battery capacity refers to the maximum volume to store charges available for discharging in the battery and is calculated by the product (Ampere · hour) of constant discharge rate (Ampere) and discharge duration (Hour) from fully charged open circuit voltage (12.8V in our case) to fully cycled cut-off voltage (10.5V in our case).

Battery capacity can vary at different discharge rates and battery aging states. The initial capacity of battery is called nominal capacity, which is given in data sheet from manufacturer. A higher discharge rate leads to a lower capacity than nominal one. And according to [12], in our system the fixed single battery capacity is estimated about 40 Ah based on battery datasheet at an average discharging rate. The process to get this estimation is shown by (3.1) [12].

The datasheet shows battery nominal capacity is C_{nom} at I_{nom} ($C_{nom}/20$) discharging rate. So we can get:

$$C_{nom} = C(I_{nom}) = \frac{K_C C_0}{1 + (K_C - 1) \left(\frac{I_{nom}}{I_{avg}} \right)^\delta}, \quad (3.1)$$

where I_{nom} is nominal battery discharge current, unit: A; C_{nom} is nominal battery capacity, unit: Ah; I_{avg} is average battery discharge current, unit: A; C_0 is fixed battery capacity responding to average actual discharge current rate, unit: Ah and K_C, δ are battery capacity empirical coefficients, constant for a given battery and an average discharge rate, unit: 1, for both. Thus we can estimate the fixed battery capacitor C_0 by (3.1).

Battery capacity is also influenced by aging, and the present battery capacity taking aging into account can be expressed by $C_{pres} = C_0 \cdot SOH$, where SOH refers to state of health and C_{pres} is present battery capacity taking aging effect into account, unit: Ah.

Here we have discussed single battery capacity used in our system. For higher supply capability and from the standpoint of simulation, we use ten batteries in serial connection and the battery supply capability reaches 2kw. In the future, for higher supply capability application scenario, we can use larger number battery group.

3.3.2 STATE OF CHARGE (SOC) & DEPTH OF DISCHARGE (DOD)

There are a lot of literatures of the definition of SOC by different authors, which make confusion. In our system the definition of SOC is the ratio of the present amount of charges stored in the battery expressed by q over the present battery capacity:

$$SOC = \frac{q}{C_{pres}}. \quad (3.2)$$

And depth of discharge (DOD) refers to how many charges have been dispatched

in percentage of the present battery capacity:

$$\text{DOD} = \frac{C_{\text{pres}} - q}{C_{\text{pres}}} = 1 - \frac{q}{C_{\text{pres}}}. \quad (3.3)$$

The high-level control requires an accurate monitoring of state of charge (SOC). Many methods for lead-acid batteries management [14-16] are available in the literature, many using cell temperature, voltage, and current measurements. And we use current integral method to track SOC online as a simple implementation.

After SGPN boots, system would calculate initial state of charge SOC_i by the following relationship with zero battery current reference and therefore no voltage drop on internal resistance:

$$\text{SOC}_i = 1 - \frac{E_{m0} - V_{\text{bat}}}{(K_E * 300)}, \quad V_{\text{bat}} \text{ unit: Volt}. \quad (3.4)$$

(3.4) is using specification data of [17]. The lead acid battery voltage can be estimated by:

$$V_{\text{bat}} = E_{m0} - K_E(273 + \theta)(1 - \text{SOC}) + I_{\text{bat}}R_{00}[1 + A_0(1 - \text{SOC})] \quad (3.5)$$

where E_{m0} , K_E , R_{00} , A_0 are battery chemical parameters and θ is battery internal temperature. I_{bat} is battery real time use current, positive charging and negative discharging, unit: A and V_{bat} is battery real time voltage, unit: volt.

Although battery internal temperature has an approximately 30°C maximum deviation from normal room temperature, it only has negligible effect on the battery voltage since K_E is very small number and 30°C is quite small comparing with 273°C constant. And when system is initialized, battery reference current is kept zero, so the I_{bat} term could also be ignored. We can compare the extreme temperature deviation and average temperature case. For single battery, $E_{m0} = 12.8\text{V}$, $K_E = 7.2\text{mV}/^\circ\text{C}$, extreme temperature 65°C and normal average temperature 35°C, we can find the expression of SOC estimation deviation $d\text{SOC}$ between two methods:

$$dSOC = \frac{E_{mo} - V_{bat}}{K_E} \left(\frac{1}{273+35} - \frac{1}{273+65} \right). \quad (3.6)$$

The maximum deviation about 9.2% lies in the case that battery is fully discharged, which can be avoided by SOC lower limit; therefore a well regulated battery assuming $V_{bat} \geq 11V$, the deviation will not exceed 7.2% and a fuller battery has even less SOC estimation deviation as V_{bat} increases. So this method is usable if we want to reduce the systems cost of additional sensing of battery temperature.

Then system estimates the varying SOC by using integration of battery current over the latest updated battery capacity C_{latest} :

$$SOC_{[n]} = SOC_{[n-1]} + \Delta SOC = SOC_{[n-1]} + \frac{I_{bat} T_s}{C_{latest}}, \quad (3.7)$$

where T_s is sampling period.

And the present battery capacity would always be updated and regarded as C_{latest} if SOC again reaches 100% by the following relationship:

$$C_{latest} = \frac{\int_{SOC_i}^{100\%} I_{bat} dt}{100\% - SOC_i}, \text{ unit: Ah.} \quad (3.8)$$

This capacity update should only occur on SOC 100% bound instead of the lower 50% bound. The reason is to minimize internal resistance influence during battery voltage sampling which this update is based on. When SOC is near 100%, the charging current is small enough, typically $C_0/40$, to ignore internal resistance influence. However, when SOC reaches lower boundary, battery current can still be as large as 20A, which would cause much larger deviation. So for a more accurate estimation, SOC is updated on 100% end.

3.3.3 STATE OF HEALTH (SOH)

State of health indicates the extent the battery capacity is close to a nominal one.

We can derive it from $C_{pres} = C_0 \cdot SOH$:

$$SOH_i = \frac{C_{latest}}{C_0} . \quad (3.9)$$

And initial state of health SOH_i is estimated based on this by substituting $C_{pres} = C_{latest}$, which means we use the latest capacity record and the fixed nominal capacity to estimate initial SOH and the latest capacity is updated every time battery is fully charged or SOC is 100%.

According to [18], we use 80% for the lower boundary of SOH as a battery's normally working range.

3.3.4 BATTERY AGING COST

Battery aging cost should be considered as a pricing variable in battery use problem. In SGPN lead acid battery use scenario, aging is primarily affected in two ways: battery internal grid corrosion and degradation. The amount of loss conducted by battery grid corrosion and degradation follows 1:4 ratio according to [19], and charging and discharging almost contribute on the same level to battery grid corrosion.

So the total battery grid corrosion effect could be ignored both for discharging and charging operations and we only calculate the discharging cost price when battery discharging.

According to [19], battery discharging aging is affected by last fully recharging interval, recent minimum discharging SOC and bad recharging cycles. "Last fully recharging interval" Δt_{SOC} is defined by the time period between now and the latest fully recharged 100% SOC state time point. And "recent minimum discharging SOC" SOC_{min}

refers to the minimum SOC during last fully recharging interval. And “bad recharging cycles” n defines the remarkable degradation effect caused by the sulfate dissolution when recharging to nearly 95% SOC level [19] also during last fully recharging interval. And also this national lab research report’s corresponding mathematic relationship formula can be described in rule-based algorithm, which uses condition judgment logic and allows more complicated mathematic expression than optimal model method we propose here. The detail relationships are as following:

$$f_{\text{SOC}} = 1 + (c_{\text{SOC}0} + c_{\text{SOCmin}} \cdot (1 - \text{SOC}_{\text{min}})) \cdot \sqrt{\frac{I_{\text{factor}}}{I_{\text{dchgnom}}}} \cdot \sqrt[3]{e^{\frac{n}{3.6}} \cdot \Delta t_{\text{SOC}}}; (3.10)$$

$$V_{\text{b_cal}} = N_{\text{bat}} \cdot (U_0 - g \cdot (1 - \text{SOC}) + \rho_d \cdot \frac{I_{\text{dchg}}}{C_n} + \rho_d \cdot M_d \cdot \frac{I_{\text{dchg}}}{C_n} \cdot \frac{(1 - \text{SOC})}{c_{\text{do}} - (1 - \text{SOC})}); (3.11)$$

$$\text{Price}_{\text{dchg}} = \text{BRC} \cdot \exp(-c_z \cdot (1 - \frac{Z_w}{1.6 \cdot \text{ZIEC}})) \cdot \frac{c_z}{1.6 \cdot \text{ZIEC} \cdot C_n} \cdot f_{\text{SOC}} / V_{\text{b_cal}} \cdot 1000; (3.12)$$

f_{SOC} is a discharging cost factor related to last fully recharging interval, recent minimum discharging SOC and bad recharging cycles;

$c_{\text{SOC}0}$ is constant slope factor of SOC, unit: h^{-1} ;

c_{SOCmin} is constant slope factor of minimum SOC, unit: h^{-1} ;

BRC is each battery’s replacement charge, unit: \$;

c_n is nominal capacity for each battery, unit: Ah;

SOC_{min} is the minimum SOC since last fully recharging;

c_z is the exponent for calculation of capacity loss due to degradation;

ZIEC is number of cycles under standard condition, indicated by battery specification;

U_0 is fully charged state cell voltage;

g is electrolyte proportionality constant V;

ρ_d is discharging aggregated internal resistance ($\text{ohm} \cdot \text{Ah}$);

M_d is charge-transfer overvoltage coefficient;

C_{d0} is discharging normalized capacity factor;

SOC is present state of charge

I_{factor} is discharging current generally average level, an experience value

I_{dchg} is actual discharging current value

Δt_{SOC} is time interval since last fully charging

Z_w is the accumulated discharging Ah through put, Ah

n is the accumulated bad recharging cycles since last fully recharging

V_{b_cal} is calculated discharging battery voltage

The above battery aging mechanism is for rule-based algorithm and is different from the aging consideration for optimal model method. To simplify the optimal model method mathematic process and satisfy the fast calculation speed requirement, we try to simplify our battery model along with its constraints. So as a constraint, battery aging would be evaluated in a much simpler way for optimal model method, by using linear aging coefficient Z stated by [20]. This coefficient treats the total aging effect linearly on discharging operation, as the following relationships:

$$\Delta SOC = \frac{I_{batdchg} T_s}{C_{last}} \quad (3.13)$$

$$\Delta SOH = \begin{cases} Z \cdot \Delta SOC, & \Delta SOC < 0 \\ 0, & \Delta SOC \geq 0 \end{cases} \quad (3.14)$$

$$\Delta Cost_{bat} = \frac{\Delta SOH \cdot BRC}{SOH_{rng}}, \text{ unit: } \$ \quad (3.15)$$

where battery health loss will only be considered when discharging ($\Delta SOC < 0$) and Z is linear aging coefficient (here in our system we use $Z = 3 \times 10^{-4}$, unit: 1) derived from battery manufacturer indicated cycle numbers.

So the discharging aging cost here can be derived by substituting (3.13) and (3.14) into (3.15) as:

$$\text{Price}_{\text{bat}} = 1000 \frac{\Delta \text{Cost}_{\text{bat}}}{\Delta E_{\text{bat}}} = 1000 \frac{\frac{\Delta \text{SOH} \cdot \text{BRC}}{\text{SOH}_{\text{rng}}}}{V_{\text{bat_avg}} I_{\text{batdchg}} T_s} = 1000 \frac{\frac{Z \cdot I_{\text{batdchg}} T_s \text{BRC}}{C_{\text{last}} \text{SOH}_{\text{rng}}}}{V_{\text{bat_avg}} I_{\text{batdchg}} T_s} = 1000 \frac{Z \cdot \text{BRC}}{V_{\text{bat_avg}} C_{\text{last}} \text{SOH}_{\text{rng}}}, \text{ unit: } \$/\text{Kwh}, \quad (3.16)$$

where I_{batdchg} is discharging current; BRC refers to battery replacement cost, which is assumed to be $100N_{\text{bat}} \$$ (N_{bat} is battery number); SOH_{rng} is battery functional working range indicated by SOH, unit: 1 and is selected by 20% according to the battery type of our system; $V_{\text{bat_avg}}$ is battery average working voltage and T_s is sampling period.

3.3.5 BATTERY USE SECURITY

There are battery use security concerns on battery charging style, charging/discharging current rate constraints and SOC range constraints. Our battery system uses double charging method to make sure that both a quick recharging and a safe charging process could be achieved. In the first charging stage, when battery voltage is lower than the lead-acid battery charging gassing limit voltage, battery is charged by constant and maximum allowed charging current I_{chglmt} to let the battery recharged as quickly as possible. The charging gassing limit voltage table is temperature dependent and shown in Table 3.1 [21], which also implies battery use should only be in T_{min} to T_{max} temperature range. Then in the second stage, after this charging gassing limit voltage reached, we use constant voltage charging right at this gassing limit value and in the meanwhile letting the charging current go down correspondingly. Finally charging ends at about $C_0/40$ charging current. In Table 3.1, “WET CELL”, “GEL”, “AGM” are battery categories of different manufacture process

TABLE 3.1 Temperature Dependent Charge Gassing Voltages [21]

TEMPERATURE		WET CELL		GEL 1 (std.)		GEL 2 (fast chg.)		AGM	
Deg (F)	Deg (°C)	Accept	Float	Accept	Float	Accept	Float	Accept	Float
120	49	12.5	12.5	13.0	13.0	13.0	13.0	12.9	12.9
110	43	13.6	12.7	13.5	13.0	14.0	13.4	13.9	12.9
100	38	13.8	12.9	13.7	13.2	14.1	13.5	14.0	13.0
90	32	14.0	13.1	13.8	13.3	14.2	13.6	14.1	13.1
80	27	14.2	13.3	14.0	13.5	14.3	13.7	14.2	13.2
70	21	14.4	13.5	14.1	13.6	14.4	13.8	14.3	13.3
60	16	14.6	13.7	14.3	13.8	14.5	13.9	14.4	13.4
50	10	14.8	13.9	14.4	13.9	14.6	14.0	14.5	13.5
40	5	15.0	14.1	14.6	14.1	14.7	14.1	14.6	13.6
30	-1	15.2	14.3	14.7	14.2	14.8	14.2	14.7	13.7

and in “GEL”, there are also standard charging and fast charging difference. “Accept”

refers to acceptable maximum charging voltage and “float” refers to the preferred charging voltage during float charging period.

Generally, many battery charging systems have a third float charging stage by keeping a constant voltage less than the gassing voltage for a manufacturer indicated float charging period for better battery safety maintenance. In SGPN system, we do not include this triple charging, since this operation requires the battery system much time to sustain

on a low charging current level but battery in our system should be ready to respond to the fluctuating real time pricing information and should keep the secure charging period as short as possible.

Another battery security issue is that battery has discharging & charging rate and SOC range restrictions based on the manufacturer's safety instruction. Deep cycle extent should be limited in order to extend battery cycle life and the relationship figure of cycle life dependent on depth of discharge and cycle frequency is shown by Figure 3.1. It is estimated that SGPN would use 300-400 battery cycles per year (here one cycle is not simply one discharge process, but an accumulated 100% discharge process, which will not happen directly in SGPN battery use but in a mathematical way. For example, battery is discharged from SOC 80% to 50%, recharged to 90%, discharged again to 50%, recharged to 95% and finally discharged to 65%. In this example, there are not three cycles, but instead the actual cycle is $(80\% - 50\%) + (90\% - 50\%) + (95\% - 65\%) = 100\%$, just one cycle. So we can estimate that the cycle number line representing our battery life can be roughly the dashed line and we choose 50% as the SOC lower boundary and thus the estimated battery life is 4-5 years.

Also there should be upper SOC boundary for battery charging concern. If a battery is near 100% SOC fully charged, it would not accept large charging current but instead shunt the surplus current, which electrolyzes water and generates dangerous gas inside battery and waste energy [14]. This potential threat can be avoided by double-stage

charging in rule-based algorithm or be avoided by a simplified SOC charging current limit function in optimal model method:

$$I_{bat} \leq 1.25 * C_0 * (1 - SOC), \text{ unit: ampere, } SOC \geq 80\% \quad (3.17)$$

When SOC is lower than 80%, battery charging limit restricts charging current

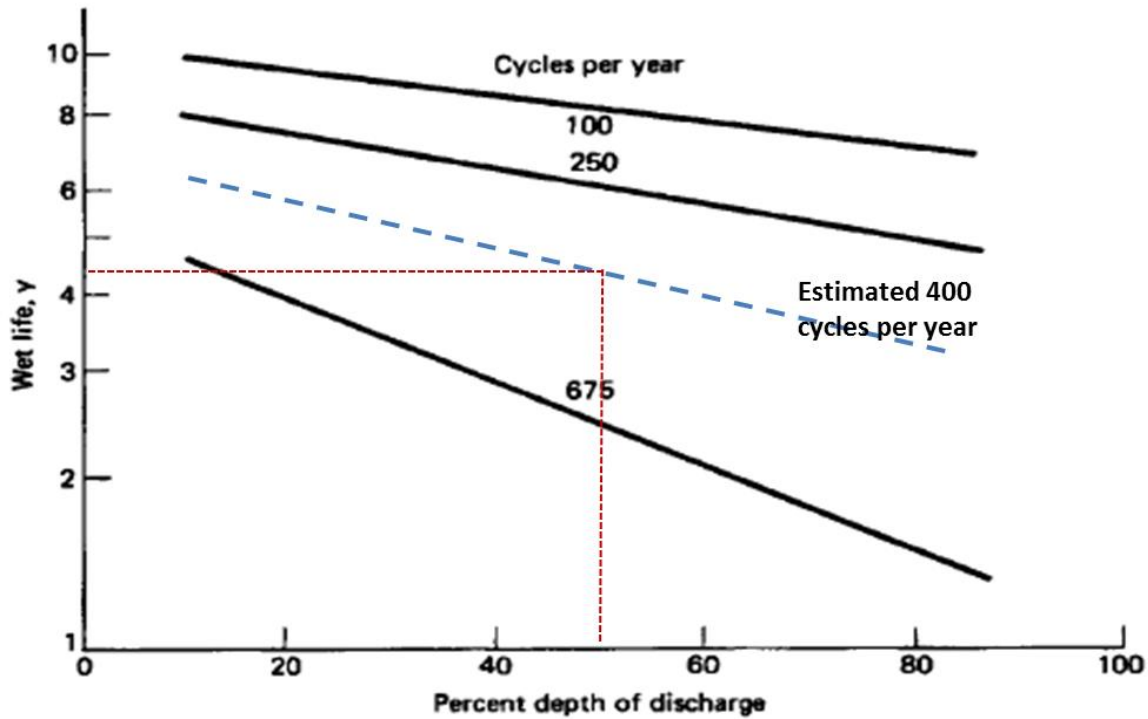


Figure 3.1 Effect of DOD and cycle number per year on wet battery at 25°C [13]

within I_{chglmt} and when SOC is higher than 80%, limit function restricts charging current within an SOC related value smaller than $C_0/4$. And this limit function method is much more conservative in optimal model than rule-based one since the battery voltage estimation accuracy in optimal model method is generally beyond security requirement of gassing voltage limit and voltage control is not applicable but is substituted by SOC control in a more conservative way in optimal model method.

Here all the safety concern for optimal model method are summed up into Figure 3.2. And the temperature security concern can only be applied by saturation operation in optimal model method, where an over or under temperature operation would be forced to stop and thus may affect the optimality effect in practical operation.

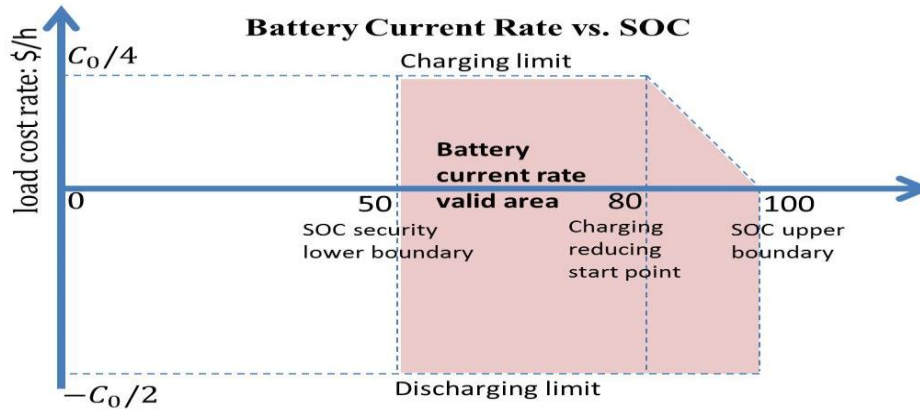


Figure 3.2 Battery use current region within constraints for optimal control method

3.4 CORE CONTROL ALGORITHM STRUCTURE

This section will explain the core algorithms structure in three operation modes: Battery Use Control, Load Switches Priority Control, Thermal Load Control and Power Flow Balance Control sequentially, which are shown in the flow chart of Figure 3.3. And the related subsystem algorithms are listed in Table 3.2.

3.5 PRICING DIRECTED BATTERY USE ALGORITHM

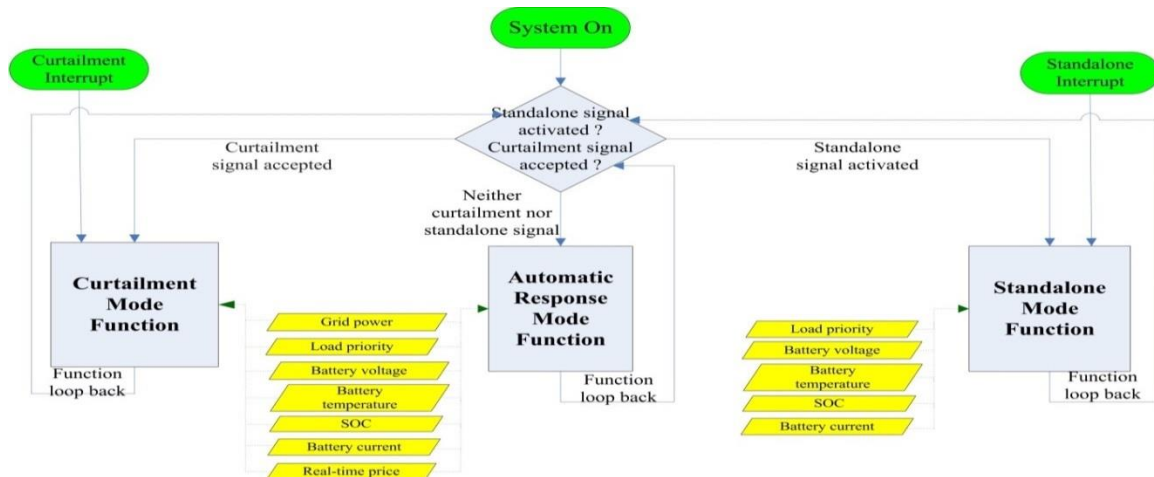


Figure 3.3 Top structure of SGPN algorithm in three modes

Table 3.2 Related core algorithms in each operation mode

Operation Mode Control Algorithm	automatic response mode	load curtailment mode	standalone mode
Pricing Directed Battery Use	✓	✓	✗
Load Switches Priority Control	✗	✓	✓
Thermal Load Set Point Control	✓	✓	✓
Power Flow Balance Control	✗	✗	✓

Battery use control is involved in the grid-connected and pricing affecting modes, typically automatic response mode and load curtailment mode. In standalone mode, batteries are forced to balance the power difference between PV generation and load consumption, so there is no scope to apply pricing directed battery rate control.

There are two options for battery use algorithm: optimal model method and rule-based algorithm. The explanation for the optimal model method will be in the form of formula and related function charts. And Rule-based algorithm will be explained by flow chart since logic expressions dominate the whole structure.

3.5.1 OPTIMAL MODEL METHOD

3.5.1.1 METHOD INTRODUCTION

The objective for the optimization problem based on optimal model is to decide

the battery charging and discharging rate schedule for a given pricing schedule and minimize the cumulative electric cost during the next 24 hour period.

One of the most difficult problems faced with the implementation of the battery control module is the effective optimization period, which means how long the optimization will last, in addition to a time efficient calculating algorithm matching the update of predictive system parameters with the accuracy of optimization in an acceptable degree. In previous efforts, rule-based algorithms such as [22] were widely used for the easiest implementation but the potential quantified effectiveness to further optimize battery usage was not explored. Other literature such as [23] presents an algorithm focusing on a short-term optimal battery schedule but does not apply to long time periods. Dynamic programming (DP) [4][24] has long calculation time (about several minutes on PC platform Matlab environment) if the total schedule lasts for 24 hours in our system case. SGPN derives an optima model and utilizes intelligent searching algorithms inside Matlab, typically interior point algorithm, which uses relatively simple math and in less than 5 seconds in the same environment computes an acceptable optimal solution for 24 hour period. The introduction of this algorithm follows this sequence: optimization model establishment, real-time updated scheduling and final results and conclusion in Chapter 4 results part.

3.5.1.2 OPTIMIZATION MODEL

In this part, the optimization objective and constraints discussed above would be converted into mathematical model expression.

The optimization target battery current rate schedule for the next 24 hours is evenly discretized into N stages, expressed as a one by N vector, I_{bat} [$1 \times N$], unit:

Ampere. Then we can derive the expressions for state-of-charge, battery voltage, battery power on corresponding stages (here we use subscript “_v” to represent a $[1 \times N]$ vector):

$$SOC_{-v} = SOC_{i_{-v}} + \frac{I_{bat_v} \frac{24}{N}}{C_0 SOH} \left[\begin{array}{cccc} 1 & 0 & \dots & 0 \\ \vdots & \ddots & \ddots & \vdots \\ \vdots & \ddots & \ddots & 0 \\ 1 & \dots & \dots & 1 \end{array} \right] \left. \vphantom{\frac{I_{bat_v} \frac{24}{N}}{C_0 SOH}} \right\} N \text{ dimension} , \quad (3.18)$$

where $SOC_{i_{-v}}$ vector has the same element of initial SOC ; C_0 is the fixed nominal battery capacity; SOH is battery state-of-health, the variation of which can be ignored during one day. This is the vector version of SOC estimation formula (3.7) and it expresses the estimated daily SOC level according to battery use schedule with $24/N$ hour time span.

According to (3.5), the lead acid battery voltage can be estimated by:

$$V_{bat_v} = E_{m0_v} - K_E(273 + \theta)(1 - SOC_{-v}) + I_{bat_v} R_{00} [1 + A_0(1 - SOC_{-v})] \quad (3.19)$$

E_{m0} , K_E , R_{00} , A_0 are battery electromotive force parameters, unit: V, $V/^\circ C$, $m\Omega$, 1, respectively. And (3.19) shows a battery voltage estimation method based on predictive SOC vector and lets the algorithm know the battery voltage at each time instant in a predictive way. As stated before, that temperature deviation would not influence battery voltage much, we can use $35^\circ C$ to indicate the average battery operation point. Battery power can be expressed by:

$$P_{bat_v} = V_{bat_v} I_{bat_v}, \text{ unit: watt} \quad (3.20)$$

Then the objective function can be expressed by:

$$F_o(I_{bat_v}) = \sum_{i=1}^{96} (f_{cost_price_i} + f_{cost_aging_i}) \quad (3.21)$$

$$f_{cost_price_i} = \begin{cases} f_{PV>Load}, P_{PV_i} - P_{Load_i} \geq 0 \\ f_{PV<Load}, P_{PV_i} - P_{Load_i} < 0 \end{cases} \quad (3.21a)$$

$$f_{cost_aging_i} = \Delta Price_{bat_i} 0.5(\text{sgn}(P_{bat_i}) - 1) P_{bat_i} \frac{24}{N}, \quad (3.21b)$$

$$\text{sgn}(x) = \begin{cases} 1, & x > 0 \\ 0, & x = 0 \\ -1, & x < 0 \end{cases}$$

(3.21) shows total battery use cost is composed of power regulation cost responding to RTP/TOU&FIT and battery aging cost. Power regulation cost can be further divided into two cases by whether PV power is greater than load power.

Cost in PV larger than load power case:

$$f_{PV>Load_v} = \text{case1}_{\text{judge}}(\text{subcase1}_{\text{judge}} \cdot \text{subcase1}_{\text{cost}} + \text{subcase2}_{\text{judge}} \cdot \text{subcase2}_{\text{cost}});$$

$$\text{case1}_{\text{judge}} = 0.5(1 + \text{sgn}(P_{PV_v} - P_{Load_v}));$$

$$\text{subcase1}_{\text{judge}} = 0.5 \left(1 - \text{sgn} \left(P_{bat_v} - (P_{PV_v} - P_{Load_v}) \right) \right);$$

$$\text{subcase1}_{\text{cost}} = \text{FIT}_{_v} P_{bat_v} \frac{24}{N};$$

$$\text{subcase2}_{\text{judge}} = 0.5 \left(1 + \text{sgn} \left(P_{bat_v} - (P_{PV_v} - P_{Load_v}) \right) \right);$$

$$\text{subcase2}_{\text{cost}} = \text{TOU}_{_v} (P_{bat_v} - P_{PV_v} + P_{Load_v}) \frac{24}{N} + \text{FIT}_{_v} (P_{PV_v} - P_{Load_v}) \frac{24}{N};$$

Case1_{judge}: $0.5(1 + \text{sgn}(P_{PV_v} - P_{Load_v}))$ indicates only if PV power larger than load power ($P_{PV_v} > P_{Load_v}$), this cost term is effective;

Subcase1_{judge}: $0.5 \left(1 - \text{sgn} \left(P_{bat_v} - (P_{PV_v} - P_{Load_v}) \right) \right)$ indicates only if battery power smaller than the surplus PV power over load power ($P_{bat_v} < P_{PV_v} - P_{Load_v}$), this cost term is effective. And in this case, battery power is charged by extra PV power and decreases the feed-in ability or is discharged to supply grid and earn more and thus increases the total cost. This cost term is decided by subcase1_{cost}: $\text{FIT}_{_v} P_{bat_v} \frac{24}{N}$.

Subcase2_{judge}: $0.5 \left(1 + \text{sgn} \left(P_{\text{bat}_v} - (P_{\text{PV}_v} - P_{\text{Load}_v}) \right) \right)$ indicates only if battery power larger than the surplus PV power over load power ($P_{\text{bat}_v} > P_{\text{PV}_v} - P_{\text{Load}_v}$), this cost term is effective. And in this case, battery power is charged by both grid and PV power, so the total cost is increased by subcase2_{cost}: $\text{TOU}_v (P_{\text{bat}_v} - P_{\text{PV}_v} + P_{\text{Load}_v}) \frac{24}{N} + \text{FIT}_v (P_{\text{PV}_v} - P_{\text{Load}_v}) \frac{24}{N}$.

Cost in PV less than load power case:

$$f_{\text{PV} < \text{Load}_v} = \text{case2}_{\text{judge}} (\text{subcase3}_{\text{judge}} \cdot \text{subcase3}_{\text{cost}} + \text{subcase4}_{\text{judge}} \cdot \text{subcase4}_{\text{cost}})$$

$$\text{case2}_{\text{judge}} = 0.5 (1 + \text{sgn}(-P_{\text{PV}_v} + P_{\text{Load}_v}));$$

$$\text{subcase3}_{\text{judge}} = 0.5 \left(1 + \text{sgn} \left(P_{\text{bat}_v} - (P_{\text{PV}_v} - P_{\text{Load}_v}) \right) \right);$$

$$\text{subcase3}_{\text{cost}} = \text{TOU}_v P_{\text{bat}_v} \frac{24}{N};$$

$$\text{subcase4}_{\text{judge}} = 0.5 \left(1 - \text{sgn} \left(P_{\text{bat}_v} - (P_{\text{PV}_v} - P_{\text{Load}_v}) \right) \right);$$

$$\text{subcase4}_{\text{cost}} = \text{TOU}_v (P_{\text{PV}_v} - P_{\text{Load}_v}) \frac{24}{N};$$

Case2_{judge}: $0.5 (1 + \text{sgn}(-P_{\text{PV}_v} + P_{\text{Load}_v}))$ indicates only if PV power less than load power ($P_{\text{PV}_v} < P_{\text{Load}_v}$), this cost term is effective;

Subcase3_{judge}: $0.5 \left(1 + \text{sgn} \left(P_{\text{bat}_v} - (P_{\text{PV}_v} - P_{\text{Load}_v}) \right) \right)$ indicates only if battery discharging power less than the excessive load power over PV power ($P_{\text{PV}_v} - P_{\text{Load}_v} < P_{\text{bat}_v}$), this cost term is effective. And in this case, battery power is discharged to supply part of the excessive load power and reduce the grid burden and thus decreases the total cost or battery is charged to add even more grid burden. However, either of both

cases shares the same cost term expression and this cost term is expressed by

$$\text{subcase3}_{\text{cost}}: \text{TOU}_{\text{v}} P_{\text{bat}_v} \frac{24}{N}.$$

Subcase4_{judge}: $0.5 \left(1 - \text{sgn} \left(P_{\text{bat}_v} - (P_{\text{PV}_v} - P_{\text{Load}_v}) \right) \right)$ indicates only if battery discharging power larger than the excessive load power over PV power ($P_{\text{bat}_v} < P_{\text{PV}_v} - P_{\text{Load}_v}$), this cost term is effective. In this case, load is supplied by both battery power and PV power and the excessive battery supply power into the grid would be taken into account by FIT. So the cost term is $\text{subcase4}_{\text{cost}}: \text{FIT}_{\text{v}} (P_{\text{bat}_v} - P_{\text{PV}_v} + P_{\text{Load}_v}) \frac{24}{N} + \text{TOU}_{\text{v}} (P_{\text{PV}_v} - P_{\text{Load}_v}) \frac{24}{N}$.

Aging cost: $f_{\text{cost_aging}} = \Delta \text{Price}_{\text{bat}_v} 0.5 (\text{sgn}(P_{\text{bat}_v}) - 1) P_{\text{bat}_v} \frac{24}{N}$ indicates that if battery discharging will lead to aging cost and charging will not have such effective cost as discharging.

Both battery use cases and all the subcases related to electricity price/FIT are show in Figure 3.4. In this figure PV and load curves are only sketches not a real data profile and the straight lines boundary of battery use subcases indicates the rough range of the battery use power instead of the exact range determined by $V_{\text{bat}} I_{\text{bat}}$.

$f_{\text{cost_aging}_v}$ refers to the battery aging cost as discharging happens.

After substitution of (3.18-3.20) into (3.21) and the parameters from battery datasheet and manipulation, we can get an objective function only related to I_{bat_v} .

And sign function “sgn” is used to empower the objective function of incorporating the comparison relationship into a mathematical formula expression. For example, $0.5(\text{sgn}(P_{\text{bat}_v}) - 1)$ tells us only if P_{bat} is negative or battery is discharging, this term is active, and otherwise it will be zero.

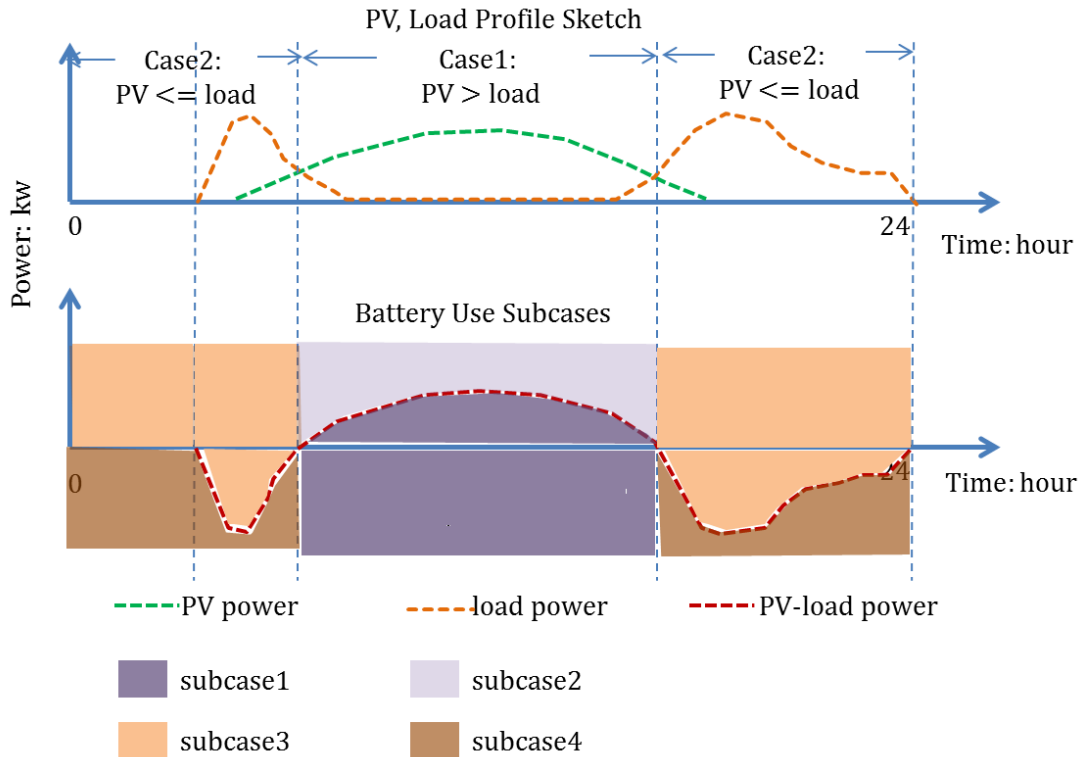


Figure 3.4 Battery use all subcases corresponding to price

By observing the form of the objective function, we find neither it nor its derivative is continuous function, which can not be used to check the convexity of the multiple arguments function or be handled by most differential parameters necessary optimization algorithms. And all these mathematic processing obstacles of that “sgn” function are due to discontinuity at origin, which causes a step hop. However, this can be conquered by an approximating alternative, by using the following mathematical expression:

$$\text{sgn}(x) \approx \text{sigmoid}(x) = \frac{2}{1 + e^{-100x}} - 1;$$

We can find how close these two functions are from Figure 3.5. And the right side of this approximation, which can be represented by function “sigmoid” is a completely

continuous and derivable function on the whole real number definition domain. Moreover, if the final optimization vector result does not have any element exactly letting the “sigmoid” function equal to zero, we can further enlarge the absolute value of the power of expectation term in the sigmoid function to make our approximation more accurate.

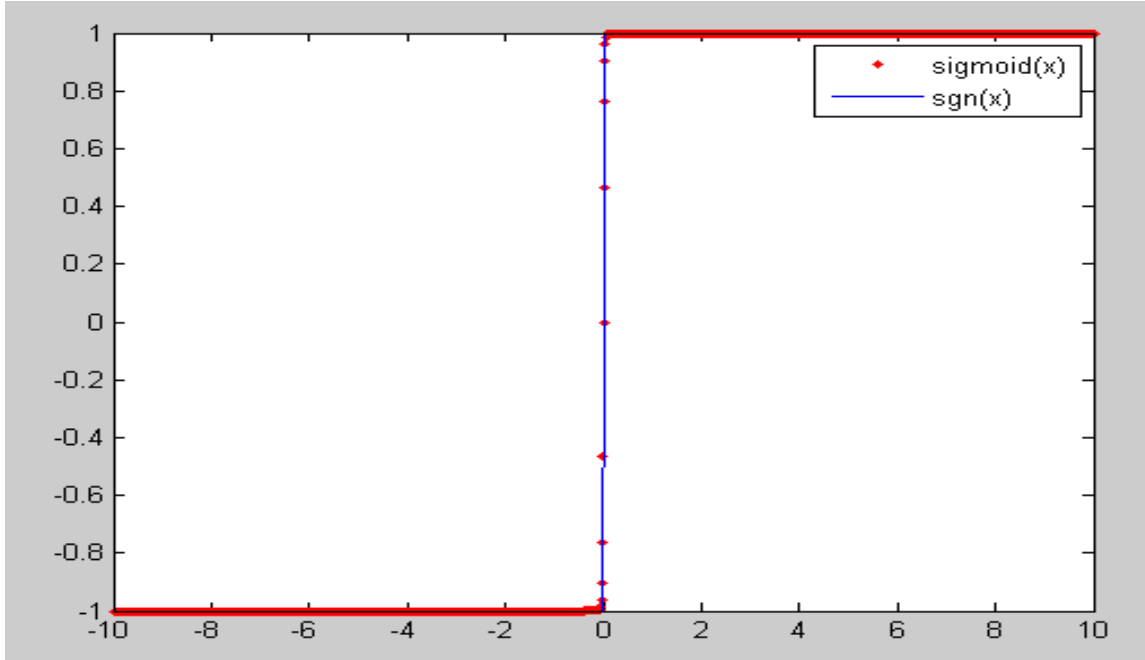


Figure 3.5 Comparison between sigmoid and sgn functions

The similar way, this sign function will work in the following several formulas.

Cost in PV larger than load power case:

$$f_{PV>Load_v} = case1_{judge}(subcase1_{judge} \cdot subcase1_{cost} + subcase2_{judge} \cdot subcase2_{cost});$$

$$case1_{judge} = 0.5(1 + \text{sigmoid}(P_{PV_v} - P_{Load_v}));$$

$$subcase1_{judge} = 0.5 \left(1 - \text{sigmoid} \left(P_{bat_v} - (P_{PV_v} - P_{Load_v}) \right) \right);$$

$$subcase1_{cost} = FIT_{_v} P_{bat_v} \frac{24}{N};$$

$$subcase2_{judge} = 0.5 \left(1 + \text{sigmoid} \left(P_{bat_v} - (P_{PV_v} - P_{Load_v}) \right) \right);$$

$$\text{subcase2}_{\text{cost}} = \text{TOU}_{\text{v}}(P_{\text{bat}_{\text{v}}} - P_{\text{PV}_{\text{v}}} + P_{\text{Load}_{\text{v}}}) \frac{24}{N} + \text{FIT}_{\text{v}}(P_{\text{PV}_{\text{v}}} - P_{\text{Load}_{\text{v}}}) \frac{24}{N};$$

Cost in PV less than load power case:

$$f_{\text{PV} < \text{Load}_{\text{v}}} = \text{case2}_{\text{judge}}(\text{subcase3}_{\text{judge}} \cdot \text{subcase3}_{\text{cost}} + \text{subcase4}_{\text{judge}} \cdot \text{subcase4}_{\text{cost}})$$

$$\text{case2}_{\text{judge}} = 0.5(1 + \text{sigmoid}(-P_{\text{PV}_{\text{v}}} + P_{\text{Load}_{\text{v}}}));$$

$$\text{subcase3}_{\text{judge}} = 0.5 \left(1 + \text{sigmoid} \left(P_{\text{bat}_{\text{v}}} - (P_{\text{PV}_{\text{v}}} - P_{\text{Load}_{\text{v}}}) \right) \right);$$

$$\text{subcase3}_{\text{cost}} = \text{TOU}_{\text{v}} P_{\text{bat}_{\text{v}}} \frac{24}{N};$$

$$\text{subcase4}_{\text{judge}} = 0.5 \left(1 - \text{sigmoid} \left(P_{\text{bat}_{\text{v}}} - (P_{\text{PV}_{\text{v}}} - P_{\text{Load}_{\text{v}}}) \right) \right);$$

$$\text{subcase4}_{\text{cost}} = \text{FIT}_{\text{v}}(P_{\text{bat}_{\text{v}}} - P_{\text{PV}_{\text{v}}} + P_{\text{Load}_{\text{v}}}) \frac{24}{N} + \text{TOU}_{\text{v}}(P_{\text{PV}_{\text{v}}} - P_{\text{Load}_{\text{v}}}) \frac{24}{N};$$

Aging cost:

$$f_{\text{cost}_{\text{aging}}} = \Delta \text{Price}_{\text{bat}_{\text{v}}} 0.5(\text{sigmoid}(P_{\text{bat}_{\text{v}}}) - 1) P_{\text{bat}_{\text{v}}} \frac{24}{N},$$

Then we need to consider constraints for this objective function:

$$I_{\text{dchg}_{\text{limt}}} \leq I_{\text{bat}_{\text{v}}} \leq I_{\text{chg}_{\text{limt}}}(\text{SOC}) \quad , \quad (3.22a)$$

or

$$I_{\text{dchg}_{\text{limt}_{\text{v}}}} \leq I_{\text{bat}_{\text{v}}} \begin{bmatrix} 1 & 0 & \dots & 0 \\ 0 & \ddots & \ddots & \vdots \\ \vdots & \ddots & \ddots & 0 \\ 0 & \dots & 0 & 1 \end{bmatrix} \leq I_{\text{chg}_{\text{limt}_{\text{v}}}}(\text{SOC}) \quad (3.22b)$$

According to (3.22b) and the Figure 3.2 battery charging current limit over SOC assumed to be f_{SOC} , we can derive and replace (3.22) by:

$$I_{\text{dchg}_{\text{limt}_{\text{v}}}} \leq \begin{bmatrix} 1 & 0 & \dots & 0 \\ 0 & \ddots & \ddots & \vdots \\ \vdots & \ddots & \ddots & 0 \\ 0 & \dots & 0 & 1 \end{bmatrix} I_{\text{bat}_{\text{v}}} \leq f_{\text{SOC}} \left(\text{SOC}_{\text{i}_{\text{v}}} + \frac{I_{\text{bat}_{\text{v}}} \frac{24}{N}}{C_0 \text{SOH}} \begin{bmatrix} 0 & 0 & \dots & 0 \\ 1 & \ddots & \ddots & \vdots \\ \vdots & \ddots & \ddots & 0 \\ 1 & \dots & 1 & 0 \end{bmatrix} \right), \quad (3.22c)$$

$$\text{SOC}_{\text{limt}} \leq \text{SOC}_{\text{v}} \leq 100\% \quad , \quad (3.23a)$$

By substitution of (3.18), we can get the transformation of constraint (3.23a):

$$\frac{C_0 \text{SOH}}{\frac{24}{N}} (\text{SOC}_{\text{Imt}} - \text{SOC}_{i_v}) \leq I_{\text{bat}_v} \begin{bmatrix} 1 & 0 & \dots & 0 \\ \vdots & \ddots & \ddots & \vdots \\ \vdots & \vdots & \ddots & 0 \\ 1 & \dots & \dots & 1 \end{bmatrix} \leq \frac{C_0 \text{SOH}}{\frac{24}{N}} (100\% - \text{SOC}_{i_v})$$

(3.23b)

So the combination of (3.22c) and (3.23b) is the constraints of this problem.

3.5.1.3 CONVEXITY JUDGMENT

There is one sort of optimization problem called convexity optimization with the local minimum the same as the global minimum, which is a very useful property to conveniently transform the global optimization problem into a local one and enable many mature methods to solve so far. So we would like to check the convexity of this problem.

According to convexity theory, the judgment of convexity of an optimization problem is composed of two parts: the convexity of the objective function and the convexity of the definition domain described by constraints.

First we try to judge convexity of the objective function. The objective function is a multi-input function and we can use Hessian Matrix for the judgment. In our problem, we use $y = f(x_1, \dots, x_{96}) = \sum_{i=1}^{96} f_i(x_i)$ to represent the objective function.

From (3.21), we know the function is the sum of 96 separate one-input functions.

Because of this linear operation feature, we can derive the Hessian Matrix to this form:

$$H = \begin{bmatrix} \frac{\partial^2 f}{\partial x_1^2} & \frac{\partial^2 f}{\partial x_1 \partial x_2} & \dots & \frac{\partial^2 f}{\partial x_1 \partial x_{96}} \\ \frac{\partial^2 f}{\partial x_2 \partial x_1} & \frac{\partial^2 f}{\partial x_2^2} & \dots & \frac{\partial^2 f}{\partial x_2 \partial x_{96}} \\ \vdots & \vdots & \ddots & \vdots \\ \frac{\partial^2 f}{\partial x_{96} \partial x_1} & \frac{\partial^2 f}{\partial x_{96} \partial x_2} & \dots & \frac{\partial^2 f}{\partial x_{96}^2} \end{bmatrix} = \begin{bmatrix} \frac{d^2 f_1}{dx_1^2} & 0 & \dots & 0 \\ 0 & \frac{d^2 f_2}{dx_2^2} & \dots & 0 \\ \vdots & \vdots & \ddots & \vdots \\ 0 & 0 & \dots & \frac{d^2 f_{96}}{dx_{96}^2} \end{bmatrix}$$

So the convexity of the objective function is determined by the convexity of the 96 single-input functions, which we will focus on next.

The form of these single-input functions are exactly the same, so we only investigate one of them which has two cases determined by the term: $P_{PV_v} - P_{Load_v}$. If we can prove single $f_i(x_i)$ function's convexity in both cases, we can prove the convexity of the whole objective function.

When PV power is larger than load power, the function can be regarded as a function with three piecewise lines smoothly connected together, shown in Figure 3.6.

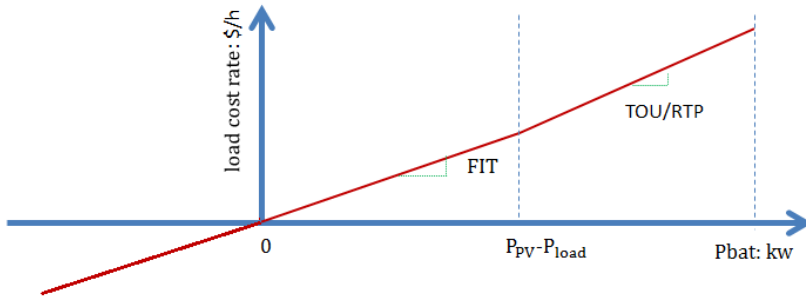


Figure 3.6 Battery use cost rate when solar power larger than load power

We can find that if TOU or RTP is greater than FIT, then the second order derivative of $f_i(x_i)$ is always larger than zero and thus the objective function is convex. Otherwise if TOU or RTP is less than FIT, the objective function is not convex and we can not apply convex optimization directly. We can divide the problem into sub-problems which guarantee the convexity of both objective function and definition domain and compare their minimums to get the global minimum. Typically this sub-problem division technique here can be adding one more constraint:

$$0 \leq P_{bat_v} = V_{bat_v} I_{bat_v} \leq P_{PV_v} - P_{Load_v}. \quad (3.24)$$

And for the other case, when PV power is less than load power, the function can be regarded as a function of two piecewise lines smoothly connected together, shown in Figure 3.7. And this time this function has the similar convexity requirement of TOU or RTP greater than FIT. If this condition does not hold, we still need a subspace division by adding the following constraint:

$$P_{bat_v} = V_{bat_v} I_{bat_v} \leq P_{PV_v} - P_{Load_v} \leq 0. \quad (3.25)$$

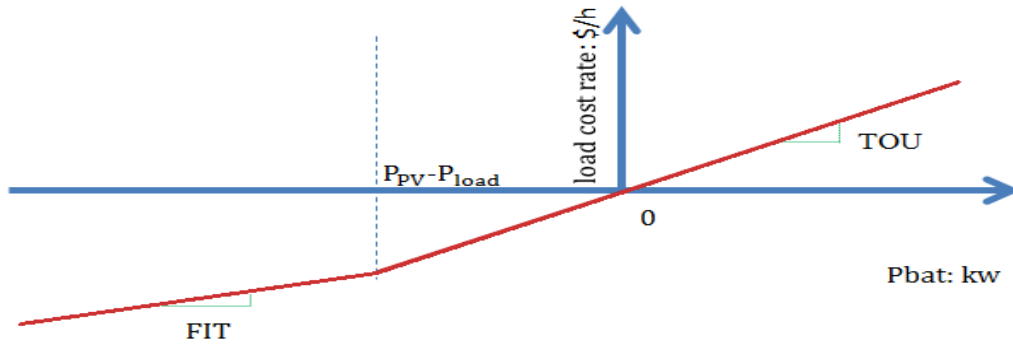


Figure 3.7 Battery use cost rate when solar power less than load power

Besides, the aging cost term is always there no matter whether it is in case 1 or case 2. And we can also find it is convex either from its function plot shown in Figure 3.8 or from the second order derivative judgment.

Then we check the convexity of definition domain defined by (3.23b). To prove

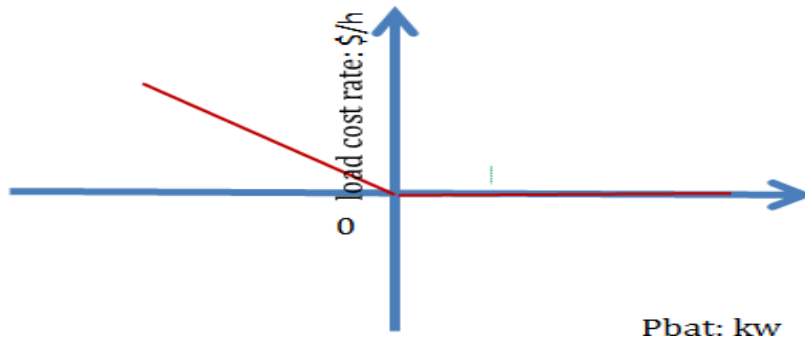


Figure 3.8 Battery aging cost rate when discharging

the convexity of the definition domain S, we do combination and transformation to the matrix expressions in (3.23b):

$$\frac{C_0 \text{SOH}}{\frac{24}{N}} (\text{SOC}_{\text{imt}} - \text{SOC}_{i_v}) = C1$$

$$\frac{C_0 \text{SOH}}{\frac{24}{N}} (100\% - \text{SOC}_{i_v}) = C2$$

$$\begin{bmatrix} 1 & \dots & \dots & 0 \\ \vdots & \ddots & \ddots & \vdots \\ \vdots & \ddots & \ddots & 0 \\ 1 & \dots & \dots & 1 \end{bmatrix} = A,$$

then (3.23b) can be substituted by matrix A, C1, C2:

$$S: C1 \leq I_{\text{bat}_v} A \leq C2.$$

Now assume there are two feasible elements x1 and x2 in S, which means the following two relationships are valid:

$$C1 \leq x1 \cdot A \leq C2$$

$$C1 \leq x2 \cdot A \leq C2.$$

We can easily derive from these two inequalities to get the following:

$$C1 = (\lambda + (1 - \lambda))C1 \leq \lambda \cdot x1 \cdot A + (1 - \lambda)x2 \cdot A \leq (\lambda + (1 - \lambda))C2 = C2$$

$$\lambda \in (0,1).$$

And this is just the definition of convexity set, so the convexity of the domain set defined by (3.23b) is proved.

In (3.22b) , the left ineuqality relationship: $I_{\text{dchg_lmt}_v} \leq I_{\text{bat}_v}$

$$\begin{bmatrix} 1 & 0 & \dots & 0 \\ 0 & \ddots & \ddots & \vdots \\ \vdots & \ddots & \ddots & 0 \\ 0 & \dots & 0 & 1 \end{bmatrix}$$

defines also a convex set similarly to the relationship S: $C1 \leq I_{\text{bat}_v} A \leq C2$ proved above.

But the right side:

$$-f_{\text{SOC}} \left(\text{SOC}_{i_v} + \frac{I_{\text{bat}_v} \frac{24}{N}}{C_0 \text{SOH}} \begin{bmatrix} 0 & 0 & \dots & 0 \\ 1 & \ddots & \ddots & \vdots \\ \vdots & \ddots & \ddots & 0 \\ 1 & \dots & 1 & 0 \end{bmatrix} \right) + \begin{bmatrix} 1 & 0 & \dots & 0 \\ 0 & \ddots & \ddots & \vdots \\ \vdots & \ddots & \ddots & 0 \\ 0 & \dots & 0 & 1 \end{bmatrix} I_{\text{bat}_v} \leq 0, \text{ we need to figure}$$

out whether it is convex.

From Figure 3.2 we can see that $-f_{\text{SOC}}(\mathbf{u})$, expressed by the “charging limit” dashed line as upper boundary, is convex and the internal term of the multiple inputs compound function is a linear combination of I_{bat_1} to $I_{\text{bat}_{96}}$, so according to the compound function convexity property, this function:

$$-f_{\text{SOC}} \left(\text{SOC}_{i_v} + \frac{I_{\text{bat}_v} \frac{24}{N}}{C_0 \text{SOH}} \begin{bmatrix} 0 & 0 & \dots & 0 \\ 1 & \ddots & \ddots & \vdots \\ \vdots & \ddots & \ddots & 0 \\ 1 & \dots & 1 & 0 \end{bmatrix} \right) + \begin{bmatrix} 1 & 0 & \dots & 0 \\ 0 & \ddots & \ddots & \vdots \\ \vdots & \ddots & \ddots & 0 \\ 0 & \dots & 0 & 1 \end{bmatrix} I_{\text{bat}_v}$$

is also a convex function and thus its level set is a convex set. Then the complete definition domain is the intersection set of the convex sets expressed by (3.22b) and (3.23c) proved above, so it is also convex.

3.5.1.4 UTILIZATION OF MATLAB ALGORITHMS

Now since the problem is convex with nonlinear objective function and constraints, we can directly use the Matlab optimization toolbox to solve this optimization problem. We use “fmincon” command, which is the assembly of several optional optimization algorithms typically for nonlinear optimization problems and these algorithms are interior-point algorithm, active set algorithm, sqp algorithm and trust-region-reflective algorithm. The result of using Matlab optimization toolbox will be shown in Chapter 4.

3.5.1.5 REAL-TIME UPDATING

The battery control module is realized by the cooperation of real-time updating sub-module and battery current reference calculation sub-module. This architecture is

dependent on the fact that the battery current reference can only be calculated by taking predictive load power, solar power, and pricing into account. So SGPN battery control works in a predictive scenario in which one time point's decision is completely dependent on how the price varies in the future and the comparison of future load and solar power. And generally accurate real-time load forecast and PV generation forecast would improve the system's real-time performance. However, because there would always be uncertain error between real-time data and prediction, it is necessary to apply a method to update and keep real-time optimal of the schedule. There are two variables with difference between real-time and predictive data: RTP and $P_{PV} - P_{Load}$.

When RTP is used to calculate cost, there would be price deviation between predictive and real price. And generally, the real-time difference between PV power and load power should be considered as main error to fix. The reason that PV power and load power is treated as an union is that only their difference is meaningful to the optimization problem, as can be seen from the expression of (3.21a). SGPN would monitor the deviation between predicted and real-time cumulative cost saving, which is caused by $P_{PV} - P_{Load}$ and/or RTP and after the deviation reaches certain threshold $Th_{\Delta cost}$, system retrieves the latest predictive inputs from internet or prediction related inputs to reschedule the battery use.

We can adjust $Th_{\Delta cost}$ to direct how frequently the updating should occur based on the algorithm's average executing time t_{cal} on different platforms. We can express the relationship as:

$$Th_{\Delta cost} \geq r_{avg_cost} t_{cal}, \quad (3.26)$$

where $r_{\text{avg_cost}}$ is the average cost deviation rate. For example, we have a personal computer Matlab environment running optima method 15 seconds once. And according to a normal situation, there will be approximately 30 cents cost deviation every hour, so the threshold should be larger than $30 \times \frac{15}{1 \times 60 \times 60} = 0.125$ cents.

3.5.2 BATTERY USE RULE-BASED ALGORITHM

There is a tradeoff between error of predictive inputs and optimization potentiality of an algorithm here for our SGPN system. If a predictive inputs algorithm is utilized, a perfect optimal result would be there if prediction exactly equals to actuality. However, in reality, there are always problems from the deviations between predictive and real-time data, which attenuate the optimization effect. On the other hand if an algorithm excludes any predictive inputs and makes decision only upon the present and/or historic data, it eliminates the probability of any input errors.

And there are two kinds of solutions for this contradiction. One is to use predictive inputs with real-time correction updated to guarantee accuracy of related predictive algorithms, such as the optimal model method mentioned before; the other is a predictive inputs excluded one, a decision making mechanism dependent only on historic and present data, such as rule-based algorithm.

Rule-based algorithm is easy to interpret and much simpler to apply by using logical judgment sentences, so it is suitable for the implementation verification and also as a counterpart to other later developed complicated algorithms.

Here in this section, the rule-based algorithm for battery use in automatic response mode is first shown, which has the same problem background and as optima method. The rule of the battery use follows two primary goals: to increase cost saving

and to keep the safety use of battery and the algorithm flow chart is also shown in Figure 3.9. And later we will show the rule-based algorithm for both load curtailment mode and standalone mode.

The flow of this rule-based algorithm follows this way. First, after system goes into rule-based automatic response mode, it checks whether the grid power is consumed or supplied by system. This is because the two grid power use cases would make difference on the battery power use price. When grid is consumed by system, more charging will increase burden to grid power, so it costs electric price. More discharging reduces grid burden power, and also has discharging aging cost, so the total discharging price is electric price minus discharging aging cost. On the other hand, when grid is

Automatic Response Mode Function (Rule-based Battery Use)

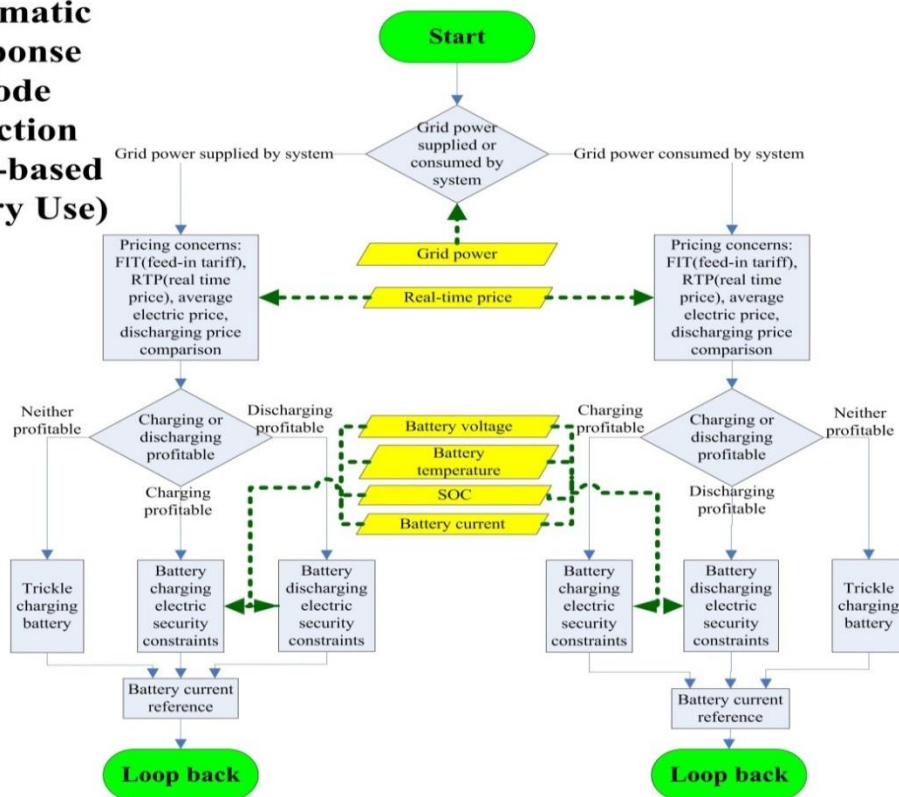


Figure 3.9 Rule-based algorithm for battery use in automatic response mode

supplied by system, more charging will reduce the capability for system to feed into grid, so it costs FIT. More discharging will increase system feeding capability, and also has discharging aging cost, so the total discharging price is FIT minus discharging aging cost.

Then, system goes to compare between the extents of the potential charging and discharging operations, based on the pricing info at this time. These extents are indicated by absolute value of the difference between charging/discharging cost and average electric price, by which the system would provide an initial battery use current reference. Finally, after system checks all the security requirements, such as battery use current rate, voltage range, SOC range and internal temperature, it determines the actually applied battery current reference. The detail control code, which also includes the rule-based algorithms for the other two modes will be attached in the final part of this chapter. The code is written in Matlab m-file format, fully commented to make everything clear and can be easily translated into Simulink code.

3.6 LOAD SWITCHES PRIORITY CONTROL

Load switches priority control is the primary load curtailment function in load curtailment mode and standalone mode. It selects and cuts off the lowest priority or most insignificant load according to user preference assigned to the system ahead.

The load switches priority control algorithm flow chart is shown in Figure 3.10. The algorithm will be started by load shutting down signal either from the average grid power over limit case in load curtailment mode or DC bus under-voltage case in standalone mode. And the two cases will not immediately trigger load shunting signal unless the cases have been sustained for a short period decided by the system response requirement, response rate and working load number. For example, if the maximum

allowed DC bus under-voltage period is 100ms and two working loads are there, then accounting for 10ms of the command transfer and actuator delay, then load shutting signal will not be enabled until DC bus under-voltage period reached $(100/2-10)=40\text{ms}$ and will keep disabled if there is only 1ms under-voltage period caused by voltage ripple on DC bus. Load number needs to be considered, since one cutting off operation may not guarantee the required load level so we use the total number of present working loads.

After system receives this load cutting enabled signal, it will find all the working loads through current sensor assigned to each load in control. And then after system gets the working loads list, it compares and finds the lowest priority load, and enables circuit breakers.

As we can see from Figure 3.10, load switches priority is the primary part of load curtailment mode and its enable signal is from the average grid power evaluation by the following relationship:

$$\text{load cutting off} = \begin{cases} \text{enabled,} & Pwr_{\text{curtl}} > Pwr_{\text{grdlimt}} \\ \text{disabled,} & Pwr_{\text{curtl}} \leq Pwr_{\text{grdlimt}} \end{cases} \quad (3.27)$$

where Pwr_{curtl} is the average grid power during load curtailment request accepted period and the calculation formula is :

$$Pwr_{\text{curtl}} = \frac{\int_{\text{curtailment start}}^{\text{time now}} Pwr_{\text{grd}} * dt}{\text{curtailment period so far}}, \quad (3.28)$$

and Pwr_{grdlimt} is the utility assigned grid power limit.

Besides, in load curtailment mode, if average grid power is under assigned limit, then no cutting off operation will be taken and just the same control style as in automatic response mode will be used.

Load switches priority control will be coded also in the final section of this

chapter in Matlab M-file.

3.7 THERMAL LOAD CONTROL

According to [6], thermal loads such as HVAC and water heater take up more than 50% of the total residential power consumption, so it is significant to explore the potential margin in thermal load control to help energy peak shaving. Although HVAC set point control margin is in $\pm 2^{\circ}\text{C}$ range around users' preference, and may not enough to curtail whole HVAC load, it will be included as auxiliary load shaving method, which means it does not affect the load switches control operations and takes effect only when

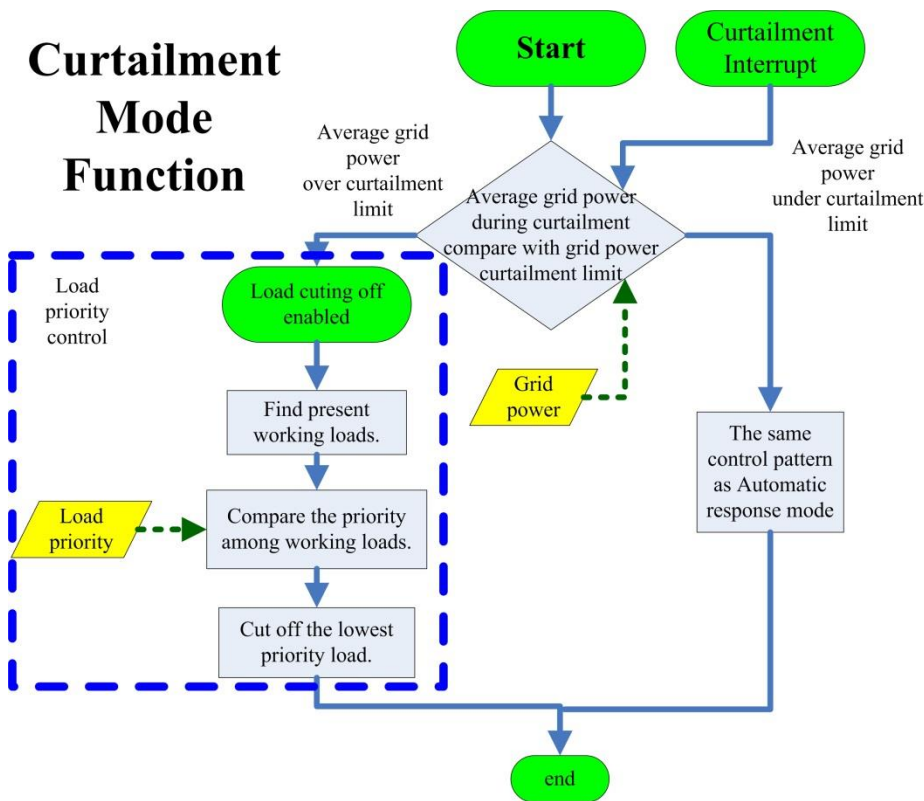


Figure 3.10 Load switches priority control algorithm flow chart

HVAC is on. Unlike Load Switches Priority Control, Thermal Load Control takes action not only in load curtailment mode and standalone mode but also in automatic response

mode as a regular load shaving and cost saving method. In this section, a HVAC control algorithm will be discussed based on the brief introduction of the principles related to air-conditioner and the building and theoretical analysis of HVAC simulation model.

There are primarily two kinds of air-condition systems dependent on the size, ductless or duct system. And we explore on the latter one, which is generally called central air-condition, since we take the thermal dynamics of the whole house as the research target. And in our system, the air-condition has the bidirectional thermal flow capability, which means both cooling and heating functions and such AC system is also called “heat pump”.

A basic AC system is composed of four parts: condensing coil, expansion valve, evaporator coil and compressor Figure 3.11.

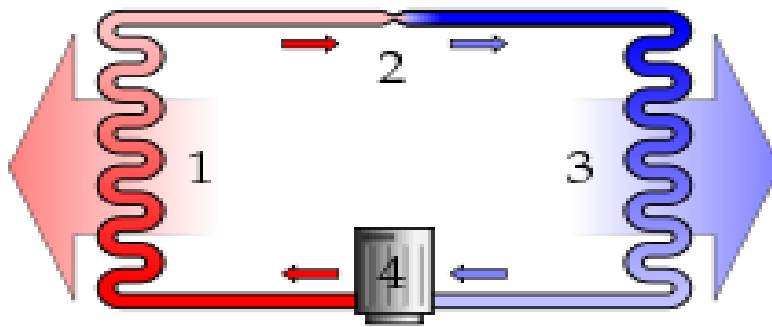


Figure 3.11 HV air-condition working principle diagram [25]

Phase change principle is used on a material with excellent thermal characteristics called refrigerant. In the cooling cycle, refrigerant gas is first compressed into high temperature and pressure liquid phase by an electrical motor and then transferred into condensing coil to dissipate heat and convert into mediate temperature and pressure liquid, where the total refrigerant thermal energy is decreased. Then liquid refrigerant passes through expansion valve and reaches evaporator coil, where refrigerant quickly

inflates into gas phase accompanying with heat absorption from indoor air, which cools our rooms. Then the gas refrigerant loops back into compression step. A heating process follows the same principle, but a reverse refrigerant flow direction.

In general, air conditions use compressor to cause pressure change, which actively condenses and pumps refrigerant. And this compressor consumes electricity energy quantitatively indicated by coefficient of performance (COP), which is defined by:

$$\text{COP} = \frac{Q}{E}, \quad (3.29)$$

where Q is the heat supplied to or removed from house rooms, and E is the electric energy consumed by the heat pump.

Heat pump stops working when temperature drops below or rise above the temperature threshold (typically $\pm 1^\circ\text{C}$) of the applied environment with a benchmark of the user's desired set point. So it is necessary to do research on heat flow pattern on heat source side and the thermal characteristics of thermal house, which has close relationship with the fluctuation pattern of indoor temperature. According to [26], the relationship can be expressed by:

$$\frac{dQ_{\text{pmp}}}{dt} = (T_{\text{pmp}} - T_{\text{in}})\dot{M}c \quad (3.30)$$

$$\frac{dQ_{\text{loss}}}{dt} = \frac{T_{\text{in}} - T_{\text{out}}}{R_{\text{thm}}}, \quad (3.31)$$

$$\frac{dT_{\text{in}}}{dt} = \frac{1}{M c} \left(\frac{dQ_{\text{pmp}}}{dt} - \frac{dQ_{\text{loss}}}{dt} \right), \quad (3.32)$$

where T_{in} is indoor temperature, T_{out} outdoor temperature, T_{pmp} the temperature of pumped air into room, R_{thm} house thermal resistance to indicate house's ability to isolate heat dissipation, Q_{loss} heat loss, Q_{pmp} heat gain generated by heat pump, M air mass

inside of house, \dot{M} the amount of pumped air into room in unit time period and c constant heat capacity of air.

This model is shown in Figure 3.12. Several related issues to be pointed out: although there may be other heat sources inside of the house, such as cooking and washing, their effect could be ignore comparing with heat pump; outdoor temperature is the average air temperature around the house and although it is fluctuating daily, this variation is quite slow and can be reated as constant in several minutes time span; the house thermal resistance is variable of the open extent of windows and doors, but in a general HVAC working scenario, we regard it a constatn with windows and doors completely closed.

We can see the simulation of HVAC model in Matlab simulink. This simulation shows the daily indoor temperature variation and HVAC electric power consumption in cooling mode and under a sinusoidal outdoor temperature condition.

We can derive the expression of several significant quantities.

The running power(HVAC has running and stopping periods and this running power is the average value on running period and the total average HVAC power is on running plus stopping period) can be estimated by:

$$P = \text{COP} \cdot \dot{M} \cdot c(T_{\text{set}} - T_{\text{pmp}}) \quad (3.33)$$

where T_{set} is the desired room temperature set point.

HVAC working and idling periods are expressed by:

$$H_{\text{on}} = M \cdot c \cdot R_{\text{thm}} \ln \frac{T_{\text{set}} + T_{\text{th}} + F_{\text{on}}}{T_{\text{set}} - T_{\text{th}} + F_{\text{on}}} \quad (3.34)$$

$$H_{\text{off}} = M \cdot c \cdot R_{\text{thm}} \ln \frac{T_{\text{set}} - T_{\text{th}} + F_{\text{off}}}{T_{\text{set}} + T_{\text{th}} + F_{\text{off}}} \quad (3.35)$$

$$F_{\text{on}} = -\dot{M} \cdot c \cdot R_{\text{thm}}(T_{\text{set}} - T_{\text{pmp}}) - T_{\text{out}} \quad (3.36)$$

$$F_{\text{off}} = -T_{\text{out}} \quad (3.37)$$

T_{out} is outdoor temperature, unit: °C;

T_{pmp} is temperature of pumped air into room, unit: °C;

R_{thm} is house thermal resistance to indicate house's ability to isolate heat dissipation, unit: °C/kw;

M is air mass inside of house, unit: kg;

\dot{M} is the amount of pumped air into room in unit time period, unit: kg/h;

c is constant heat capacity of air, unit: kwh/(kg · °C);

T_{set} is desired room temperature set point, unit: °C;

H_{on} is heat pump working period, unit: h;

H_{off} is heat pump idling period, unit: h;

F_{on} is heat pump working on factor, unit: °C;

F_{off} is heat pump working off factor, unit: °C.

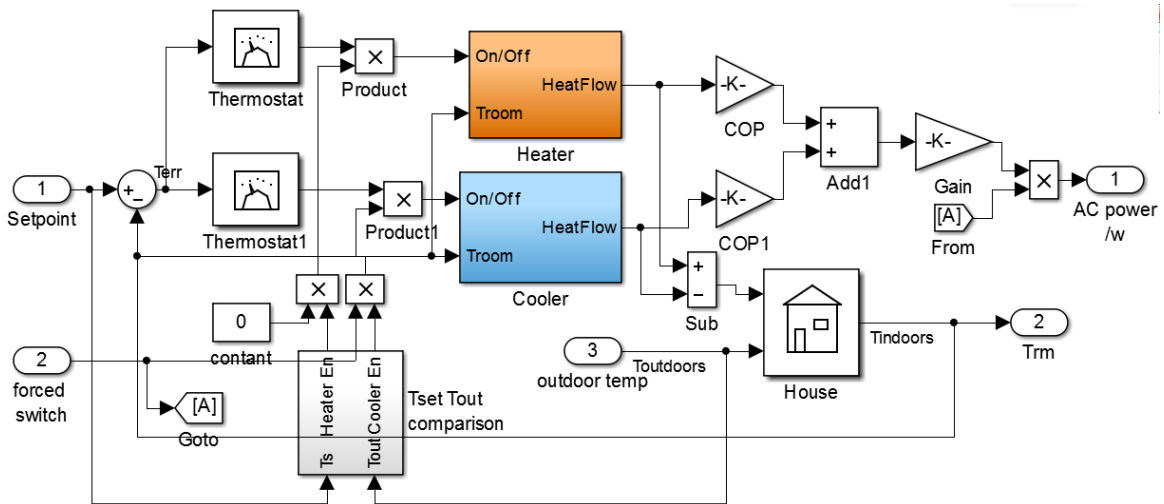


Figure 3.12 HVAC Simulink model with both heating and cooling functions

And we can also intuitively see the parameters in above expressions from room temperature and HVAC power curves shown in Figure 3.12 and Figure 3.13.

Although when HVAC starts, there is huge instantaneous current into the compressor coil to establish the magnetic field about 5-7 times as the stable starting current, it can be ignored in the analysis of the total electricity energy loss since it lasts for less than one second and also it doesn't change load's peak feature since HVAC is generally the dominant load even without this spike. Generally in standalone mode this large current consumption load would be cut off immediately after it is started, however

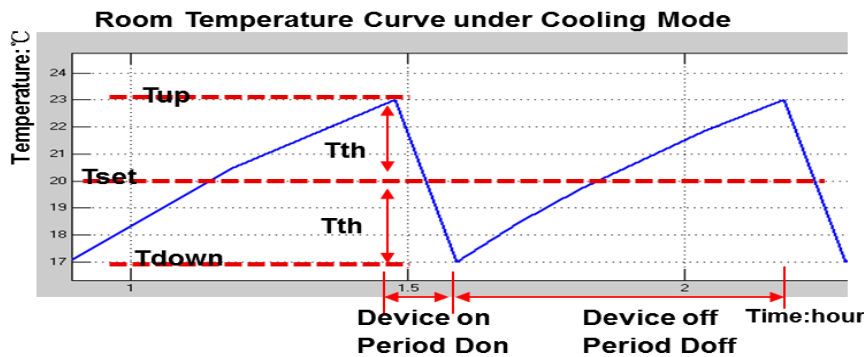


Figure 3.13 Room temperature curve under cooling mode

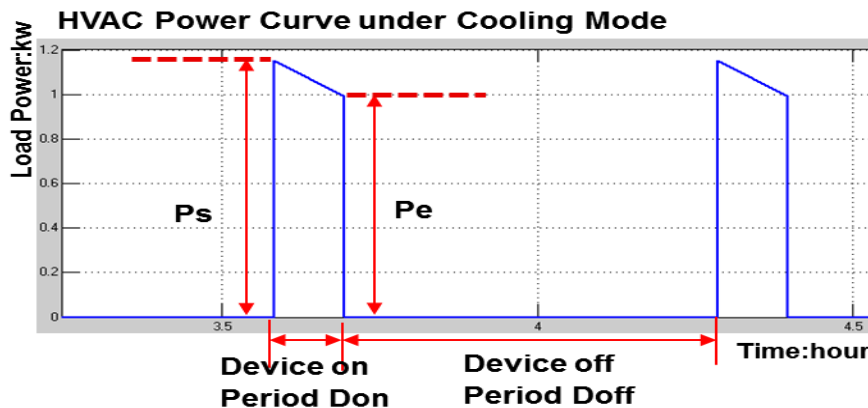


Figure 3.14 HVAC power curve under cooling mode

lead acid battery could supply huge amount of current unless it causes overheating and gasing problems, and this current would not consume much energy to damage battery. So we can use a special care on the load management channel connected with such kind of huge current starting loads, and allow a second-level excessive discharging current rate.

Base on (3.34)-(3.37), we can derive the average HVAC working power expressed by:

$$P_{HVAC} = P \frac{H_{on}}{H_{on} + H_{off}} = COP \cdot M_{rate} c(T_{set} - T_{pmp}) \frac{\ln \frac{T_{set} + T_{th} + F_{on}}{T_{set} - T_{th} + F_{on}}}{\ln \left(\frac{T_{set} + T_{th} + F_{on}}{T_{set} - T_{th} + F_{on}} \cdot \frac{T_{set} - T_{th} + F_{off}}{T_{set} + T_{th} + F_{off}} \right)} \quad (3.38)$$

The HVAC power control margin upon a set point control margin can also been estimated based on this relationship. We can estimate the control power margin for HVAC is about 100w, if we assume a 35°C outdoor temperature, 26°C desired set point and 2°C set point control margin in a house with a general parameter air-condition and room thermal isolation. This is not an impressive control margin but considering that air-condition has usually a long working period, we can expect a considerable cost saving.

The detail realization of the HVAC thermal load control is mapping the set point control percentage in the control margin to the cost rate. We use a proportional function:

$$T_{set\%} = a_t \cdot \text{cost rate} + b_t \text{ and } dT_{set} = T_{mrg} \cdot T_{set\%} \quad (3.39)$$

mapping relationship to apply more set point control at high cost rate period and less control at low cost rate period. This will be coded separately from the three mode code part and in thermal load control subsystem of the Matlab simulink environment since it does not tell operation mode difference.

3.8 POWER FLOW BALANCE CONTROL

Power flow balance control is exclusively in standalone mode, since in this mode system is disconnected to grid, which acts as a natural power balance source in automatic response mode and load curtailment mode. The difference of load control between standalone mode and load curtailment mode is in standalone mode, system requires a real time power balance between solar power source, battery usage and load usage, so system should monitor DC bus voltage and respond very fast to cut off overrate loads in millisecond for voltage bus current balancing. And also battery use related issues, such as SOC too low and too high, have considerable effect on control style and require related operation. In standalone mode, system controls its DC bus voltage by a PI controller and the device action rules. The standalone mode load control algorithm flow chart is shown in Figure 3.14. And in this mode, since there is a strict power balance requirement, so all the loads user wants to run need to be regulated by SGPN control channels.

The control target is the DC voltage bus system, which could be expressed by the differential equation:

$$C_{dc} \frac{dV_{dc}}{dt} = I_{dc}, \quad (3.40)$$

where C_{dc} is DC bus capacitance, V_{dc} is DC bus voltage and I_{dc} is DC bus current.

After the discretization, we get:

$$V_{dc}(k+1) = V_{dc}(k) + \frac{T_s}{C_{dc}} I_{dc}(k) \quad (3.41)$$

T_s is sampling period.

And we use Backward Euler discrete PI controller to track DC bus voltage and get $I_{dc}(k)$ control input:

$$dI_{dc}(k) = (K_p + K_p * K_I * T_s) * (V_{dc}(k) - V_{dcref}) - K_p * (V_{dc}(k-1) - V_{dcref}), \quad (3.42)$$

where $dI_{dc}(k)$ is the required DC bus current increment present time interval, K_p is PI

proportional parameter, K_I is PI integral parameter and $V_{dc\text{ref}}$ is DC bus voltage reference.

Both PI parameters require a real field tuning other than the Simulink tuning in Matlab.

Since DC bus current control input has a relationship with PV, load and battery current as:

Standalone Mode Function

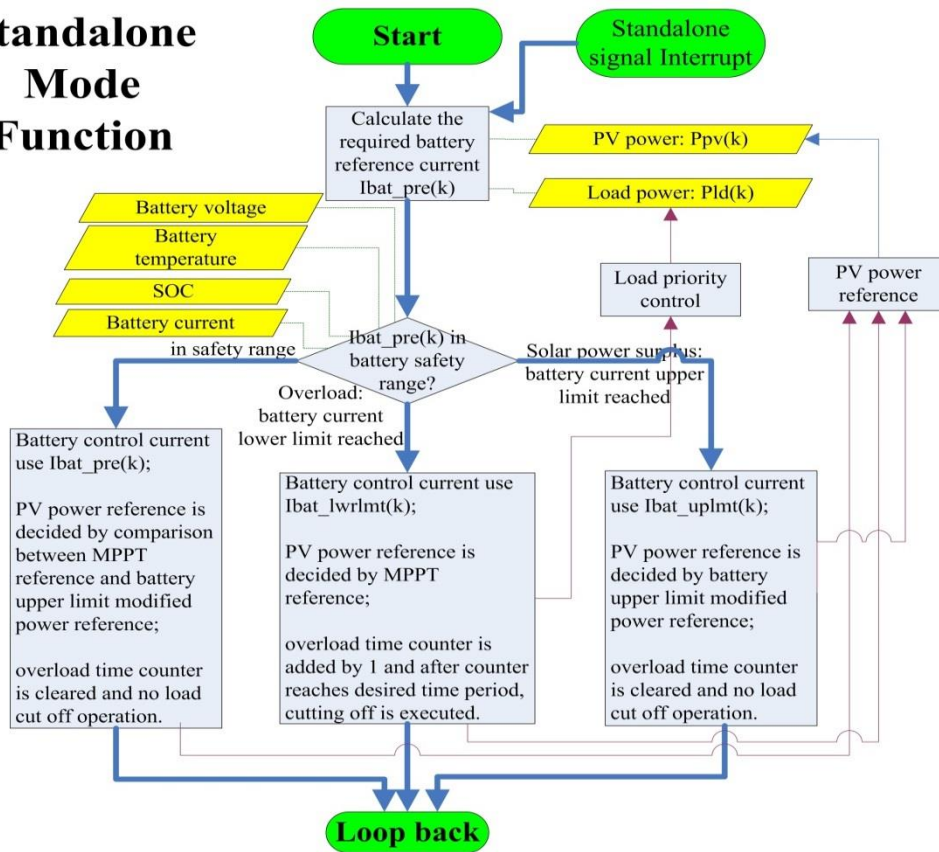


Figure 3.15 Power flow balance control algorithm flow chart for standalone mode

$$dI_{dc}(k) = dI_{pv}(k) - dI_{ld}(k) - dI_{bat}(k), \quad (3.43)$$

we would like to regulate all these current components to satisfy $dI_{dc}(k)$ requirements by rule-based algorithm in standalone mode.

We need to know what kind of control is required for each component current, which can be shown in Table 3.3. Then all these requirements are organized in rule-based

algorithm.

First, the algorithm pre-calculates the required battery current based on present and previous PV current & power, present load current and required DC bus current:

$$I_{\text{batpre}}(k) = dI_{\text{batpre}}(k) + I_{\text{bat}}(k - 1) = \left(dI_{\text{pv}}(k) - dI_{\text{ld}}(k) - dI_{\text{dc}}(k) \right) +$$

$$I_{\text{bat}}(k - 1) = \left(I_{\text{pv}}(k) - I_{\text{pv}}(k - 1) \right) - \left(I_{\text{ld}}(k) - I_{\text{ld}}(k - 1) \right) - dI_{\text{dc}}(k) + I_{\text{bat}}(k - 1);$$

(3.44)

Then this pre-calculated value is compared with battery safety concern rules, which synthesizes the present battery temperature, SOC range, charging/discharging current limit and current limit implied by charging style to judge whether this current reference

Table 3.3 Required control for current of all components in standalone mode

Component Current	Control Requirement in standalone mode
PV current	Follow maximum power point tracking (MPPT) when battery has enough power storage; disable MPPT and track battery & load power sum when battery & load power sum less than solar power.
load current	Cut off load according to load priority if DC voltage keeps decreasing for an indicated duration while both battery reaches maximum supply capacity and PV uses MPPT.
battery current	Concern battery use safety, which includes battery temperature, SOC range, charging/discharging current limit and current limit implied by charging style.

value is safe, over the safety upper limit or under the lower limit. After that, it will apply control action on battery current reference, PV current reference and load switches. The detail action for each case is shown here.

If pre-calculated battery current is safe, then algorithm would use this battery current as present battery control signal $I_{bat}(k) = I_{bat_pre}(k)$. It also tries to use maximum PV power into the system in the next interval since there is still scope of storing more solar energy into battery and so it compares the battery use upper limit related PV power with the MPPT PV power reference:

$$P_{pvref}(k+1) = \min \left(MPPT_{PVref}(k+1), P_{pv}(k) + V_{dc}(k) \left(I_{batuplmt}(k) - I_{batpre}(k) \right) \right); \quad (3.45)$$

$P_{pvref}(k+1)$ is PV power reference in the next interval and it can get PV current reference in the next interval by:

$$I_{pvref}(k+1) = \frac{P_{pvref}(k+1)}{V_{dc}(k+1)}; \quad (3.46)$$

$MPPT_{PVref}(k+1)$ is MPPT calculated PV power reference for next interval; $P_{pv}(k)$ is present PV power; $I_{batuplmt}(k)$ is present battery current upper limit value translated on DC bus side and it varies by system parameters like temperature, SOC range, as mentioned before, so this variation is expressed by time variable k ; term $P_{pv}(k) + V_{dc}(k) \left(I_{batuplmt}(k) - I_{batpre}(k) \right)$ shows how much PV power is required to fully charge the battery and make maximum use of battery storage.

And finally in this case load is not cut and time counter for cutting off operation is cleared: $N_{counter}(k+1) = 0$.

Another battery use safety case is if pre-calculated battery current under

$I_{batlwr\text{limt}}(k)$, which means battery has been using maximum discharging capability, then algorithm would keep using this upper lower current input as present battery control signal $I_{bat}(k) = I_{batlwr\text{limt}}(k)$. Similar to $I_{batup\text{limt}}(k)$, $I_{batlwr\text{limt}}(k)$ is present battery current lower limit value translated on DC bus side and it also varies by system parameters like SOC range, so this variation is also indicated by time variable k . In this case, we use MPPT PV power reference to make full use of solar power supply capability:

$$P_{pvref}(k + 1) = MPPT_{PVref}(k + 1). \quad (3.47)$$

In the meanwhile, the algorithm tries to monitor the duration of this case by time counter $N_{counter}(k + 1) = N_{counter}(k) + 1$ and if $N_{counter}(k + 1) * T_s > T_m$, the load priority cutting off operation is taken, and here T_m is the maximum system allowed under-voltage time duration.

The final battery use safety case is if pre-calculated battery current over $I_{batup\text{limt}}(k)$, then algorithm would use this upper limit current input as present control signal $I_{bat}(k) = I_{batup\text{limt}}(k)$. It also tries to control PV power to track the sum of load and battery charging power to avoid surplus solar power unbalancing system.

$$P_{pvref}(k + 1) = \min \left(MPPT_{PVref}(k + 1), P_{ld}(k + 1) + V_{dc}(k)I_{batup\text{limt}}(k) \right); \quad (3.48)$$

And also in this case load is not cut and time counter for cutting off operation is cleared: $N_{counter}(k + 1) = 0$.

3.9 RULE-BASED ALGORITHM CODE

Here the rule-based algorithm code for three operation modes is posted. This code is written in Matlab M file format and the notation part is started by duplicated percentage signs “%%”.

```
%%%%%%%%%%%% SGPN Control High Level Code %%%%%%%%%%
```


charging voltage, current and discharging current and voltage are always in safety area. This is much more robust than only use SOC to guarantee battery safety.

To synthesize all the concerns about battery, the battery use code follows these concerns: 1. Grid power situation judgment; 2. Battery use price situation; 3. Battery electrical states.

Rule-based algorithm allows more complicated description of battery aging.

According to [19], battery aging is affected by last fully recharging interval, recent minimum discharging SOC and bad recharging cycles factor.

Battery aging parameters by battery spec or from battery technology reference [17][19].

Later, battery manufacturers are supposed to provide more detail info for smart battery management.

$cSOC0 = 6.614E-5$; Constant slope for SOC factor (h^{-1})

$cSOCmin = 3.307E-3$; Impact of the minimum SOC on SOC factor (h^{-1})

$BRC = 100$; each battery replacement fee

$Cn = 40$; nominal capacity for each battery, Ah

$cz = 5$; Exponent for calculation of capacity loss due to degradation

$ZIEC = 500$; Number of cycles under standard condition;

$U0 = 2.1$; fully charged state cell voltage, V

$g = 0.076$; electrolyte proportionality constant V

$roud0 = 0.699$; discharging aggregated internal resistance ($ohm \cdot Ah$)

$Md = 0.0464$; charge-transfer overvoltage coefficient

$Cd0 = 1.75$; discharging normalized capacity factor

```

%%% SOC is present state of charge

%%% SOCmin is the minimum SOC since last fully recharging

Ifactor= -20; %%% normalized reference current for current factor

Idchgnom = -15; %%% discharging current level in

fSOC = 1 + (cSOC0+cSOCmin*(1-
SOCmin))*sqrt(Ifactor/Idchgnom)*(exp(n/3.6))^(1/3)*deltatSOC;

Vb_cal = Nbat*(U0 - g* (1-SOC) + roud0 * Idchgnom/Cn + roud0*Md*Idchg/Cn*(1-
SOC)/(Cd0-(1-SOC)));

%%% calculated discharging battery voltage

price_dchg = BRC*exp(-cz*(1-Zw/1.6/ZIEC))*cz/1.6/ZIEC/Cn*fSOC/Vb_cal*1000;

%%% deltatSOC; time interval since last fully charging

%%% Zw is the accumulated discharging Ah through put, Ah

%%% n is the accumulated bad recharging cycles since last fully recharging

if SOC <= 0.5

%%% Battery state of charge level is too low and be forced to be charged

    if Tbat >= Tmin && Tbat <= Tmax

%%% Only in this temperature, charging is allowed for battery use safety concern, and

%%% the battery charging voltage limit is dependent on battery temperature through

%%% table looking up. Battery average electrolyte temperature data are expected here.

        if Vbat < Vconst_T

            Iref = Ichglmt;

%%% Voltage under limit, fast charge battery to above 50% SOC state,

%%% by maximum charging current

```

```

else

%%% Battery voltage is no less than voltage reference, then charging is not allowed.

Iref = 0;

end

else %%% charging not allowed for inappropriate temperature

Iref = 0;

end

elseif (SOC > 0.6)||((SOC <= 0.6 && SOC0506 == 0.6)

%%% In this SOC range, battery can be either charged or discharged, dependent on price

%%% info.

if Id_pv < 0 %%% Load power minus solar power less than zero.

Prc_chg = FIT; %%% charging cost price

%%% Charging will reduce solar feeding-in capability, so it costs FIT.

Prc_dchg = FIT - p_dchg; %%% discharging earn price

%%% Discharging will lead to more feeding-in power, but also discharging aging cost,

%%% so the total discharging price is FIT minus discharging cost. In our algorithm,

%%% negative grid power is defined as grid fed by system situation. In this situation,

%%% the feeding in power can be from solar source and/or battery power. According to

%%% present regulation, power from battery should not be used to feed into the grid for

%%% FIT. However, for future application, this policy may be changed to fully satisfy

%%% residential power purchase/sale marketing requirement. So in this version battery

%%% can be controlled to discharge and feed grid.

if Prc_chg < Price_avg %%% charging profitable

```

Calculate and judge whether charging is profitable.

In this case, charging would first take up the solar feed-in capability which costs

FIT and then the charging amount above total solar power would extra cost

electric price of this time, so we compare between FIT, present price and

average electric price during one day estimated by historic data.

Average price is the daily average calculated by $Price_{avg} = \frac{\int_0^{24h} Price * dt}{24h}$. Only

when charging price lower than this price we charge battery and when price

is over average price plus the potential discharging price we can discharge battery

and in this way, guarantee every unit energy stored into battery will successfully

get cash earned.

when FIT and present price both less than average price charging is profitable and

only restricted by the maximum charging power limited of the battery for safety

and aging concern. To keep a charging battery safe and charge as fast as possible,

we use triple charging method, with battery voltage and current thresholds for each

charging stages' boundary condition.

if $Price \leq Price_{avg}$ max charging

if $T_{bat} \geq T_{min} \ \&\& \ T_{bat} \leq T_{max}$

charging allowed in appropriate temperature zone

if $V_{bat} < V_{const_T}$ charging allowed for safe voltage

rapid charge - 1st stage Voltage under limit, fast charging allowed, 1st stage of

charging V_{const_T} is linearly looked up through charging limit voltage table-

temperature and used to guide charging without obvious gassing inside battery.

if $1000 * (-I_{d_pv}) - ((Price_{avg} - FIT) * I_{ch_gmt} / dd) * V_{bat} > 0$

$$I_{ref} = (Price_avg - FIT) / dd * I_{chglmt};$$

%% According to FIT and price, decide how much the charging current is used, which
 %% is an advanced method than simply using max charging when charging profitable.
 %% “dd” is the downside price variation value. “(Price_avg-FIT)/dd” indicates how
 %% profitable present charging is and directs how much charging current be used.

else

%% If battery charging power is large enough to let grid supplying system. The actual
 %% used battery charging current will be a quadratic relationship with FIT and price
 %% and is calculated by following code.

$$poly = [1000 - ((Price_avg - Price) * I_{chglmt} / dd) * V_{bat} \\ - I_{d_pv} * (FIT - Price) * I_{chglmt} * V_{bat} / dd];$$

$$r = \text{real}(\text{roots}(poly));$$

$$rt = (r >= 0) * r;$$

$$I_{ref} = 1000 * rt / V_{bat};$$

end

$$\text{else } \% \% \% V_{bat} \geq V_{const_T}$$

%% Battery voltage is no less than voltage reference, then charging current is limited.

%% Constant voltage charging-2nd 3rd stage

$$I_{ref} = (K_{p1} + K_{p1} * K_{i1} * T_s) * (V_{bat} - V_{const_T}) + K_{p1} * (V_{batp} - V_{const_T}) + I_{batp};$$

%% backward discrete filtering PID control is used for constant voltage maintenance.

%% K_{p1} – proportional value of constant voltage control

%% K_{i1} – integral value of constant voltage control

%%

```

%% Ts – discrete PID sampling period

%% Nv – PID filtering enhancing number

%% Vbat,Vbatp – battery voltage of present and adjacent past instants

%% All these parameters need a real field tuning, although such tuning could be done
%% to fit Matlab simulation environment, however, Matlab use very easy
%% mathematic description of the real system, and could not exactly match the case
%% when real field tuning implemented.

    end

    if Iref < 0

%% the calculated battery charging current reference should be within [0,Ichglmt]

        Iref = 0 ;

elseif Iref > Ichglmt

        Iref = Ichglmt;

    end

    else %% battery temperature not in safety range, no charging

        Iref = 0;

    end

    else %% price is large enough to limit charging

%% Reuse price charging code as above, but put one more price charging limit
%% afterward.

        Iref = Price_charging();

        Plmt_prc_chg = -Id_pv*(FIT-Price)/(Price_avg-Price);

        Ilmt_prc_chg = Plmt_prc_chg*1000/Vbat;

```

```

%%% Additional charging current limit put by large enough price
Iref = min(Ilmt_prc_chg,Iref);

%%% Compare the new constraint and the original calculated one and get the
%%% discharging current reference.

    end

    elseif Prc_dchg > Price_avg %%% discharging profitable discharge according to
%%% how profitable discharging is

    Iref = (Prc_dchg-Price_avg)/du*Idchglmt;

%%% According to FIT and price, decide how much discharging current is used, which
%%% is also an advanced method than simply using maximum discharging when
%%% discharging profitable. “du” is the upside price variation value. “(Price_avg-
%%% FIT)/dd” indicates how profitable present discharging is and directs how much
%%% discharging current should be used.

    else %%% neither profitable, do not use battery

    Iref = 0;

    end

else %%% load power no less than solar power

    Prc_chg = Price; %%% cost

    Prc_dchg = Price - p_dchg; %%% earn

%%% Charging will increase more burden to grid power, so it costs electric price.

%%% Discharging will reduce grid burden power, but also cause discharging aging cost,

%%% so the total discharging price is electric price minus discharging cost.

    if Prc_chg < Price_avg %%% charging profitable

```

```

%%% Reuse price charging code as above

Iref = Price_charging();

elseif Prc_dchg > Price_avg %%% discharging profitable
if 1000*(-ld_pv)-((Prc_dchg-Price_avg)*Idchglmt/du)*Vbat<=0

Iref = (Prc_dchg-Price_avg)/du* Idchglmt;

%%% Discharging price directed discharging, the same as above discharging case.

else

poly = [1000 ((FIT-p_dchg-Price_avg)*Idchglmt/du)*Vbat -ld_pv*(FIT-
Price)*Idchglmt*Vbat/du];

r = real(roots(poly));

rt=(r<=0)*r;

Iref = 1000*rt/Vbat;

%%% Discharging power is large enough to feed grid and causes a quadratic relationship
%%% between price and discharging current.

end

if FIT < Price_avg

%%% FIT is small enough to put one more constraint on battery discharging current.

Plmt_FIT_dchg = -ld_pv*(Price-FIT)/(Price_avg-FIT+p_dchg);

Ilmt_FIT_dchg = Plmt_FIT_dchg*1000/Vbat;

Iref = max(Ilmt_FIT_dchg, Iref );

%%% Compare the new constraint and the original calculated one and get the
%%% discharging current reference.

end

```

```

else %%% neither profitable, do not use battery

    Iref = 0;

end

end

else %%% SOC <= 0.6 && SOC0506 == 0.5

%% To avoid battery charged to above 50% area and then immediately be discharged
%% responding to present price info, battery is forced to be charged onto 60% by a
%% small current when discharging profitable and a large current when charging
%% profitable. The sign "SOC0506" indicates the present SOC recently arrives at 50%
%% instead of 60% to verify this case valid.

if Id_pv < 0 %%% Load power minus solar power less than zero.

    Prc_chg = FIT; %%% charging cost price

%% Charging will reduce solar feeding-in capability, so it costs FIT. Here only
%% charging is considered, if price indicates discharging operation, do not use battery

    if Prc_chg < Price_avg

%% Reuse price charging code as above

        Iref = Price_charging();

        else %%% discharging profitable or neither profitable

            Iref = 0;

        end

    else %%% Load power no less than solar power

        Prc_chg = Price;

        if Prc_chg < Price_avg

```

%%% Reuse price charging code as above

Iref = Price_charging();

else %%% discharging profitable or neither profitable

Iref = 0;

end

end

else %%% voltage threshold not satisfied, so charging is also not allowed

Iref = 0;

end

else %%% charging not allowed for inappropriate temperature

Iref = 0;

end

else %%% Curtl signal 1(only 0/1 logic value), system in load curtailment mode

%%% In load curtailment mode, system is still connected to grid power source,

%%% but the difference is in this mode, the average grid power over time should

%%% be less than Pwrcurtl, where the calculation is :

$$%%% PWR_{curtl} = \frac{\int_{curtailment\ start}^{time\ now} Pwr_{grd} * dt}{curtailment\ period\ so\ far}.$$

%%% If average grid power lower than curtailment requirement, the system

%%% operation would have no difference from in automatic response mode.

%%% And automatic response mode is reused in the function form:

%%% Iref = AutoRspn(). However, when the average grid power reaches the limit

%%% requirement, and battery discharges maximum or battery not secure to do

%%% any discharging, we just execute load cutoff, according to user's preference

```

%%% load priority.

%%% Update curtailment energy and average grid power use value

    Egrid = Egridpre + dt*Pwrgrid;

    Pavggrid = Egrid/t;

    if Pavggrid < Pwrcurtl %%% average grid power no exceeding limit

%%% Reuse automatic response mode function code.

        Iref = AutoRspn()

    else %%% average grid power exceeding limit

%%% We first try to use battery discharging to reduce grid burden, however

%%% when this is not available to use or not enough to reduce, we cut off load

%%% after short delays (require real field system response speed test).

        if Pwrgrid > 0 %%% grid is supplying system, battery is used to do potential

%%% discharging, this is the same as in automatic response mode, so reuse the

%%% function code

            Iref = AutoRspn_Pwrgrd_ovr0();

        else %%% Grid is feeded by solar power, battery can only be used to do

%%% potential charging. In this case, the difference between that in automatic

%%% response mode is, here an additional grid power limit is applied. So we

%%% compare and use the small limit to guarantee both limit satisfied.

            Pwrchggrdlimt = abs(Pwrgrd)*(Price-FIT)/(Price-Price_avg)- abs(Pwrgrd);

%%% the price directing charging power limit

            Pwrchgcurtllmt = Pwrcurtl -Pwrgrd

            Pwrchglmt = min(Pwrchggrdlimt, Pwrchgcurtllmt)

```

```

%%% compare and use smaller limit value, then reuse other function as in automatic
%%% response mode.

Iref = AutoRspn_Pwrgrd_undr0();

end

%%% judge whether load is necessary to be cut

if Pavgrid > Pwrcurtl

    counter = counterp + 1; %%% cutoff delay judgment

else

    counter = 0; %%% clear cutoff delay

end

    if counter >= 10 %%% 10 is used to allow delay cutoff, and
%%% need real field tuning to determine practical use value

        cut_en = 1; %%% load cutoff enabled

    end

end

case 0 %%% grid is off, system works in standalone mode

%%% standalone mode is quite different from the above two modes since it is
%%% disconnected with grid, an obvious different physical environment. There would
%%% be no grid power flow in this mode. And there are three control required and
%%% controllable components in this mode: battery current reference; load switches and
%%% solar panel MPPT use. The key of maintaining the system running in this mode is
%%% to monitor the DC bus voltage and use DC voltage PI controller to make sure it is
%%% around the nominal value with maximum ripple of 5%.

```

```

Vdc_ref = 36; %%%set DC bus reference voltage (in our simulation 36V is used)

dInet = (Kp2+Kp2*Ki2*Ts)*(Vdc-Vdc_ref)-Kp2*(Vdcp-Vdc_ref);

%% DC bus voltage uses PI control to calculate the necessary DC bus current variation
%% in the next sample interval. Kp2,Ki2 are DC bus voltage related PI controller
%% parameters, which are also needed to be tuned in real system.

Iref = 0; %%% default reference battery current zero

%% If no judgment battery current reference is triggered, this value is used.

if dInet > 0 %%% DC bus undervoltage

%% next necessary DC current variation is positive, which means DC bus is less than
%% reference value and needs positive net current to balance.

Ipv_out = Ipv;

%% in this mode solar current is controlled, but in this case, no surplus solar power
%% exists, so keep MPPT open and use maximum input solar power.

counter1 = counter1p;

%% Use undervoltage state counter to calculate the undervoltage time for potential
%% load cut off operation.

cut_en = 0;

%% Initially keep load, do not cut until time counter reaches threshold.

dIbat = -Vdc_ref*(dInet-(Ipv-Ipv_a)+dIld)/Vbat;

Ibat = Ibatp + dIbat; %%% potential battery current

%% Assume load and solar power not controlled, purely control battery to achieve DC
%% current variation

if Ibat < Idchgmt

```

```

        bat_lwr = 1;

        Iref = Idchglmt;

    %%% Judge whether controlled battery current reach lower boundary. If so, use lower
    %%% boundary and set lower boundary reach sign "bat_lwr".

        end

        if SOC <= 0.5 || (SOC <= 0.6 && SOC0506 == 0.5)

    %%% If SOC is less than 0.5 or larger than 0.5 less than 0.6 from 0.5 previously, battery
    %%% is only used for charging and lower boundary sign is set.

            if Ibat < 0

                bat_lwr = 1;

                Iref = 0;

            end

        end

        if Vbat < Vconst_T

            if Ibat > Ichglmt

                bat_upr = 1;

                Iref = Ichglmt;

            end

        else

            Iref_up = (Kp1+Kp1*Ki1*Ts)*(Vbat-Vconst_T)-Kp1*(Vbatp-Vconst_T)+Ibatp;

            if Ibat > Iref_up

                bat_upr = 1;

                Iref = Iref_up;

            end

        end
    
```

```

        end
    end
    if Tbat < Tmin || Tbat > Tmax
        if Ibat > 0
            bat_upr = 1;
            Iref = 0;
        end
    end
end

%%% Battery current upper boundary check. If boundary reached, use upper boundary
%%% and set upper boundary sign.

    if bat_lwr == 0 && bat_upr == 0
        %%% If pre-calculated battery current reference reaches neither upper nor lower
        %%% boundary, just use the calculated value.
        Iref = Ibat;
    end
    if bat_lwr == 1
        counter1 = counter1p + 1;
        %%% If lower boundary reached, add undervoltage time counter by 1.
    end
    if counter1p >= 2
        cut_en = 1;
        %%% If undervoltage time counter reaches 2, enable cut-off.
        counter1 = 0;
    end

```

```

%%% clear undervoltage counter

    end

    if bat_upr == 1

        dIpv = (Iref-Ibatp)*Vbat/Vdc_ref+dInet+dIld;

        Ipv_out = Ipv_a + dIpv;

    %%% If battery current reaches upper boundary, use upper boundary battery current
    %%% and control solar power in the meanwhile to achieve DC bus current variation.

    end

    else %%% dInet <= 0 DC bus overvoltage

        cut_en = 0; %%% Do not cut load when overvoltage

        counter1 = 0; %%% clear undervoltage counter

    %%% In standalone mode, battery current reference function code reuse

        Iref = Ibat_stdaln_reuse();

        if bat_upr == 1

            dIpv = (Iref-Ibatp)*Vbat/Vdc_ref+dInet+dIld;

            Ipv_out = Ipv_a + dIpv;

        %%% If battery current reaches upper boundary, use upper boundary battery current
        %%% and control solar power in the meanwhile to achieve DC bus current variation.

        end

    otherwise %%% grid information is unknown, wait and no control operation executed

        %%% At DSP programming scenario, here we can use delay commands.

    end %%% Rule-based algorithm ends.

```

CHAPTER 4

SYSTEM SIMULATION & RESULTS

4.1 SIMULATION DIAGRAM

The purpose of the simulations is first to make sure that both rule-based and optima model method are effective for SGPN system with cost saving achievable and all system parameters such as battery current, voltage and SOC are in safety states and second to compare between enhanced rule-based algorithm and general rule-based algorithm on the capability to save more. By using rule-based algorithm, all the three SGPN modes are simulated to verify rule-based algorithm is applicable for the whole system functions.

This simulation is running in Matlab 2013a Simulink environment and the full system diagram is shown in Figure 4.1. In this diagram, SGPN system, controller, load group, utility information and measurement observers are all included and designated by tags. To give a more clear description, SGPN system represents SGPN hardware part: PV, batteries, inverter/rectifier and other converters. Controller will be applied by both rule-based and optima model methods. Load group is composed of seven kinds of profiled common household application devices: HVAC, lighting, cooking, washing, refrigerator and small electronics group, each connected with a load switch for curtailment and standalone mode load control. Utility information provides electric price and load curtailment requests, which are prescheduled data instead of real-time ones. Measurement observers are Matlab Simulink scope components.

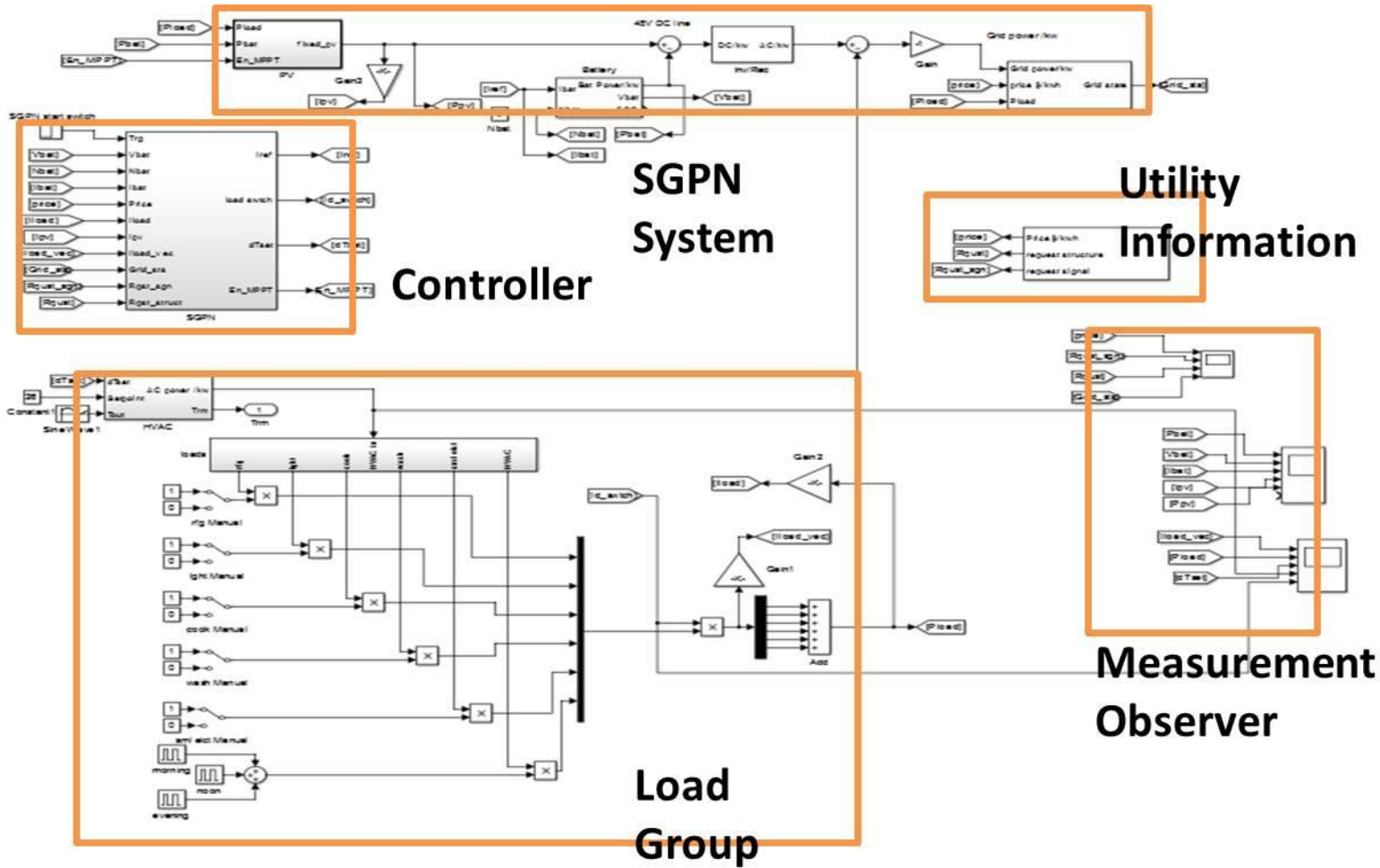
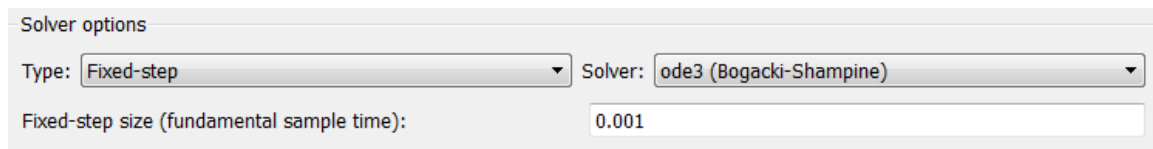


Figure 4.1 SGPN Simulink block diagram

4.2 SIMULATION PARAMETERS

Most of the parameters in this simulation are based on academic references or technique specification [9] [17-21] for components, like: lead-acid battery, photovoltaic panel. Other parameters are either from industrial/residential practice, like TOU price and load profile, or based on ideal assumptions. The simulation is assumed to be on July 1st, a summer day and it is also assumed that all the SGPN hardware components are lossless and all the parameters related to the swap of three different system modes are known one day ahead and no changes is made to these scheduled events, which is a theoretically ideal situation.

Here the simulation configurations are shown in Figure 4.2. The simulations are implemented for three operation modes on typical price and load, solar power profile to show the system can work well in all three modes and “ode3” simulation solver with sampling period 0.001hour (3.6second) is adopted to solve the discrete states model.



Solver options

Type: Fixed-step Solver: ode3 (Bogacki-Shampine)

Fixed-step size (fundamental sample time): 0.001

Figure 4.2 Simulation parameters

4.3 SIMULATION RESULTS

The simulations are separated into three sections for three operation modes. The first one is for automatic response mode and uses both optimal model method and rule-based algorithm as two main methods. Then for load curtailment mode and standalone mode, we both use rule-based algorithm.

In the first section's simulation, the model adopted by optimal model method is

different from that adopted by rule-based algorithm in two ways: it does not integrate battery internal temperature safety constraint and it uses linear aging coefficient, a different aging calculation method from that of rule-based algorithm. Both of the two differences are based on approximation and due to the highly complicated form of optimization objective function not satisfying convexity requirement, so optimal model method and rule-based algorithm can not be compared using the same benchmark. However, we can compare optimal model used case with no such battery control used case to check how much this algorithm could achieve in cost saving. And general rule-based algorithm and enhanced rule-based algorithm are using the same battery model, so they will be compared along with the battery control not used case.

The TOU and FIT pricing profiles for optimal model method are shown in Figure 4.3 and the battery use current and voltage along with solar power and load power profiles are shown in Figure 4.4.

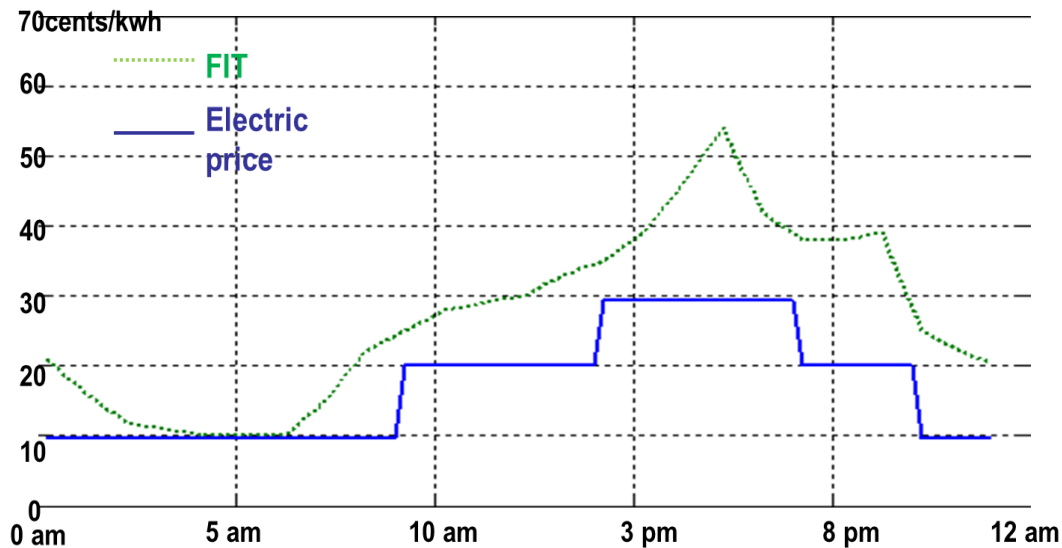


Figure 4.3 Electric price and FIT profiles for optimal model method

The other algorithm used for automatic response mode is rule based algorithm, which adopts a more complicated solar power and load power profiles. The solar power is superposed on disturbances, which are seen to have some concave parts on the “Solar Power” plot to simulate the real solar power fluctuation, for instance, caused by clouds covering. And load profile adopts refrigerator usage, which is composed of a series of spikes in the “Load Power” plot. The FIT and electric price data shown in Figure 4.5 is from the synthesized data of related real-time pricing system and can be changed to any other profile. And we use two comparison counterparts: general rule-based algorithm (in Figure 4.6) and enhanced rule-based algorithm (in Figure 4.7).

The other two sections’ simulations are for load curtailment mode (shown in Figure 4.8 and Figure 4.9) and standalone mode (shown in Figure 4.10), which are both realized by rule-based algorithms.

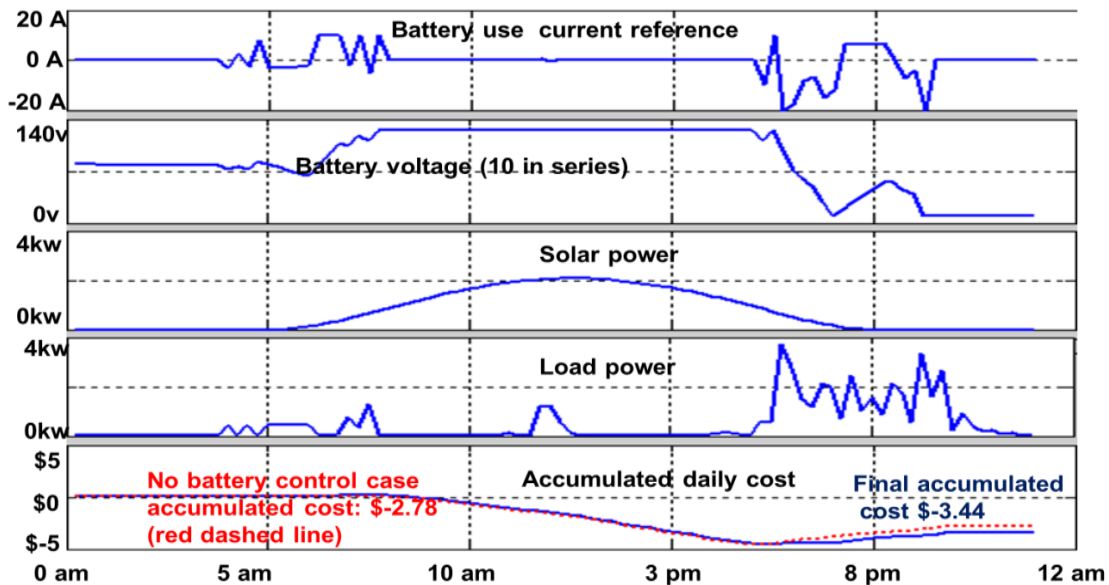


Figure 4.4 Battery current & voltage, solar & load power and daily accumulated cost in optimal model method



Figure 4.5 Electric price and FIT profiles for rule-based algorithm

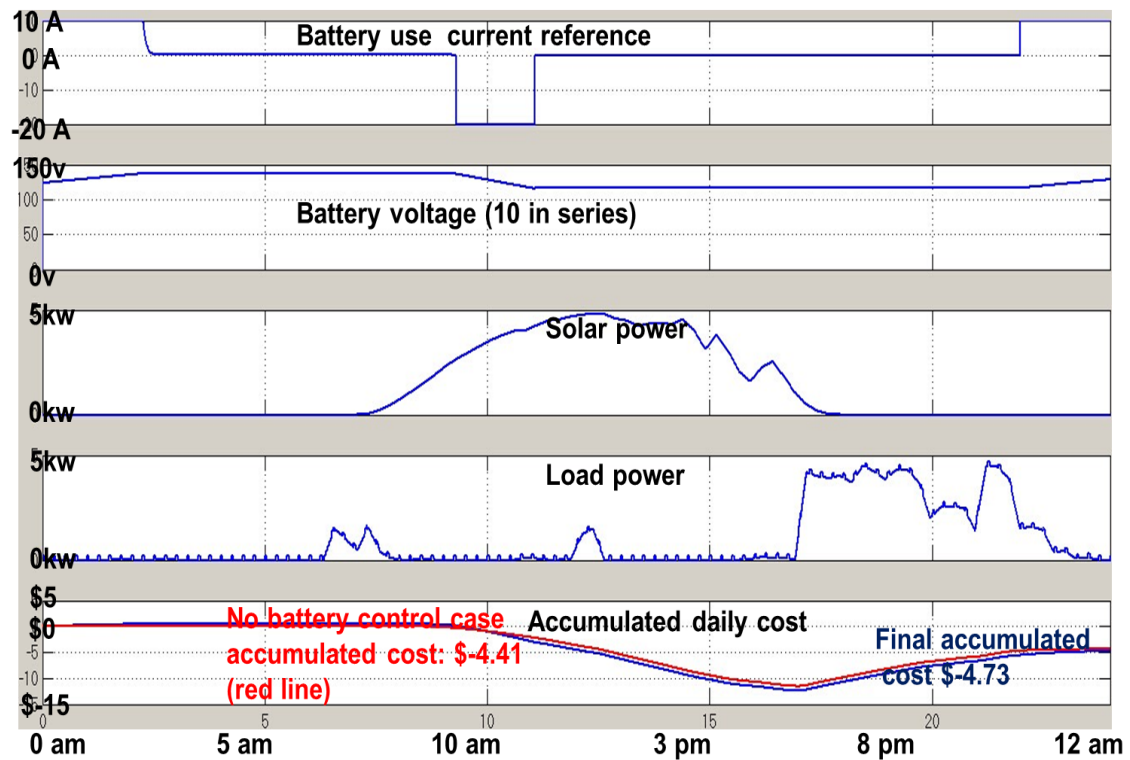


Figure 4.6 Battery current & voltage, solar & load power and daily accumulated cost in general rule-based algorithm

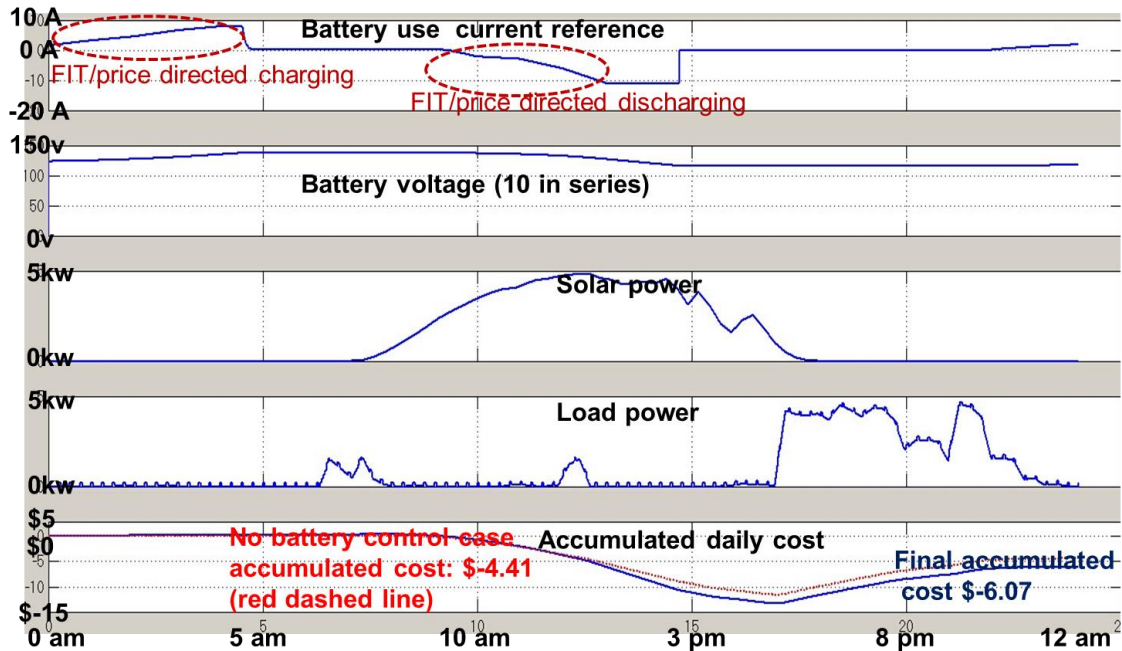


Figure 4.7 Battery current & voltage, solar & load power and daily accumulated cost in enhanced rule-based algorithm

4.4 RESULTS ANALYSIS

In the optimal model method's simulation Figure 4.4, we can see battery current and voltage are in safety area and this optimal model method enables our system an accumulated cost saving of \$ -3.44, which means we can earn \$3.44 one day by applying optimal model battery use control comparing with the battery control not used case only \$ 2.78. This result verifies that optimal model method can save money for our system and also guarantee the battery current and voltage safety requirements.

Then we compare the cost saving capability during 24 hours between enhanced rule-based algorithm and general rule-based algorithm. The former considers how profitable of present FIT and electric price to decide corresponding battery use current but the latter simply decides battery use upon whether it is profitable time period without

detecting how profitable it is.

We use the same solar and load power profile and same FIT and electric price data for the comparison. The daily accumulated cost for a battery control not used case is \$-4.41, which means we can earn \$4.41 one day by solar power's unregulated feeding into grid. On the other hand, the final accumulated daily earn is \$4.73 for general rule-based (GRB) algorithm used case and \$6.07 for enhanced rule-based (ERB) algorithm used case. This demonstrates that both algorithms are capable of earning money and especially the enhanced rule-based algorithm can earn more. From the corresponding battery current control plots we can find how this difference yields. At the beginning and in the end of the day, when FIT and electric price is getting lower, GRB tends to charge battery with maximum charging current, however, ERB calculates how profitable present charging price is, and assigns less battery charging current when profit not remarkable and more current when price info shows more profit. And in the middle of the day, when FIT is getting higher, GRB uses maximum discharging, which depletes all the stored battery energy to earn money; while on the other hand, ERB intelligently monitors FIT, judges how profitable the present discharging operation is and applies less discharging when FIT is not high enough. In both ways, ERB guarantees more money earned for the whole system.

In the second section's simulation, the simulation for Load curtailment mode is executed to check whether grid power can be controlled under a specific average level and whether the load cutting off subsystem functions normally. Since load curtailment happens only when load is larger than solar power, we focus our simulation on the period around load curtailment period.

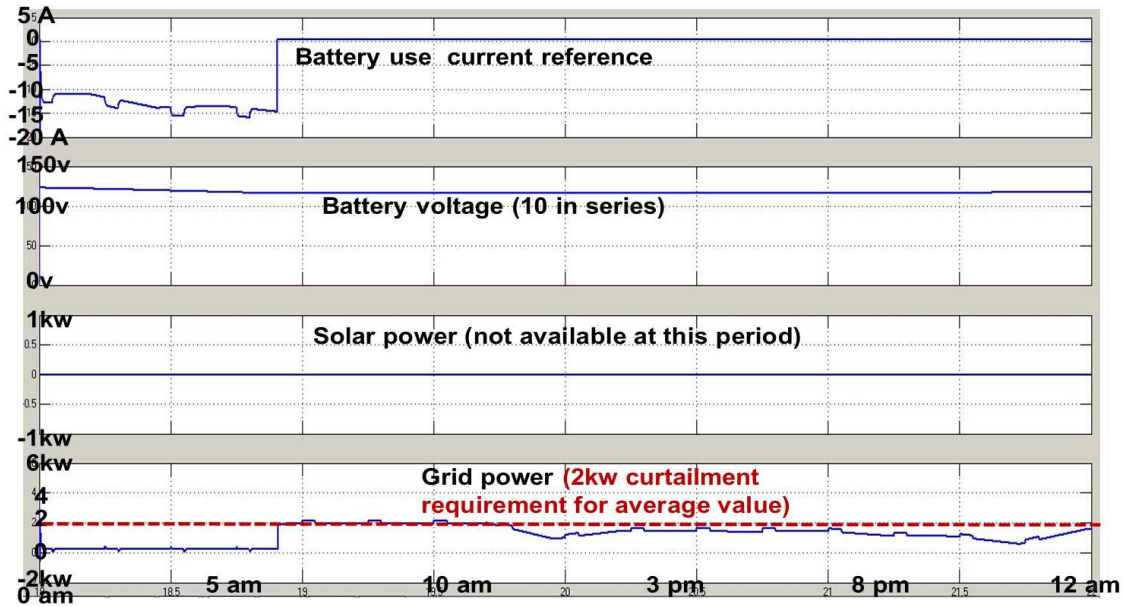


Figure 4.8 Load curtailment mode battery current & voltage, solar power & grid power

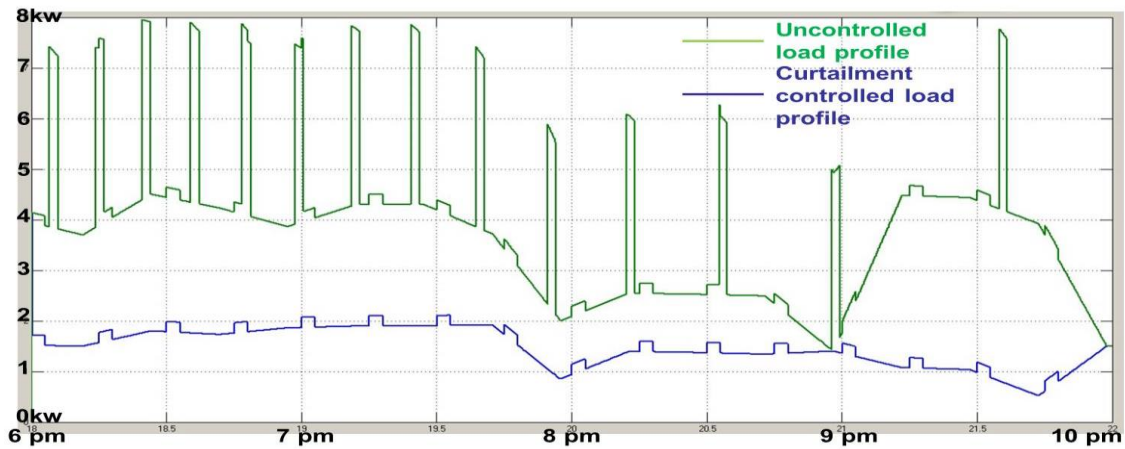


Figure 4.9 Load curtailment mode uncontrolled, controlled load profiles

From the simulation Figure 4.9, we can see during the curtailment period, solar power is in outage, and the uncontrolled load power is almost twice as much as the indicated curtailment request 2kw level. At the beginning of this period, system detects

the average grid power has exceeded the required level, so it immediately executes cutting off, and we can see the large spikes and triangular shaped load are removed in the controlled load profile and in the meanwhile, battery is trying to compensate the dominating load. After that, the rest of working load is not huge enough to increase average grid burden to be above 2kw, which keeps the curtailment successfully completed shown in Figure 4.8.

The final section's simulation is for standalone mode. Unlike the previously two modes, system in this mode is disconnected with grid, which is a more complicated physical operation environment, since the DC bus voltage of the system is sensitive to the current flow variation of PV panel, battery and load without grid's natural power balance. So a DC bus PI controller is adopted here and guarantees the DC bus voltage stable can be achieved by battery current control, PV input control and load shunt.

From the last subplot, we can see that DC bus voltage is kept around reference value, and there are only two small DC voltage drops around 4am time point and 7:30am time point, which are caused by overload and load cutting off operation. At around 4am, when there is no solar input, the spike is too large for battery to supply, the system first tries to use maximum battery discharging supply but the undervoltage is still continued for a short interval and then cutting off is executed, and we can see the spikes in the original uncontrolled load plot are removed from controlled load plot. And later from 6:30am to 7am battery is capable to supply load without solar input but at around 7:30am, battery is depleted and forced to charge or not use, however at that time, solar power can't solely supply load, so load is cut off for a second time and battery is charged by solar power. When solar power gets larger and reaches the maximum charging power

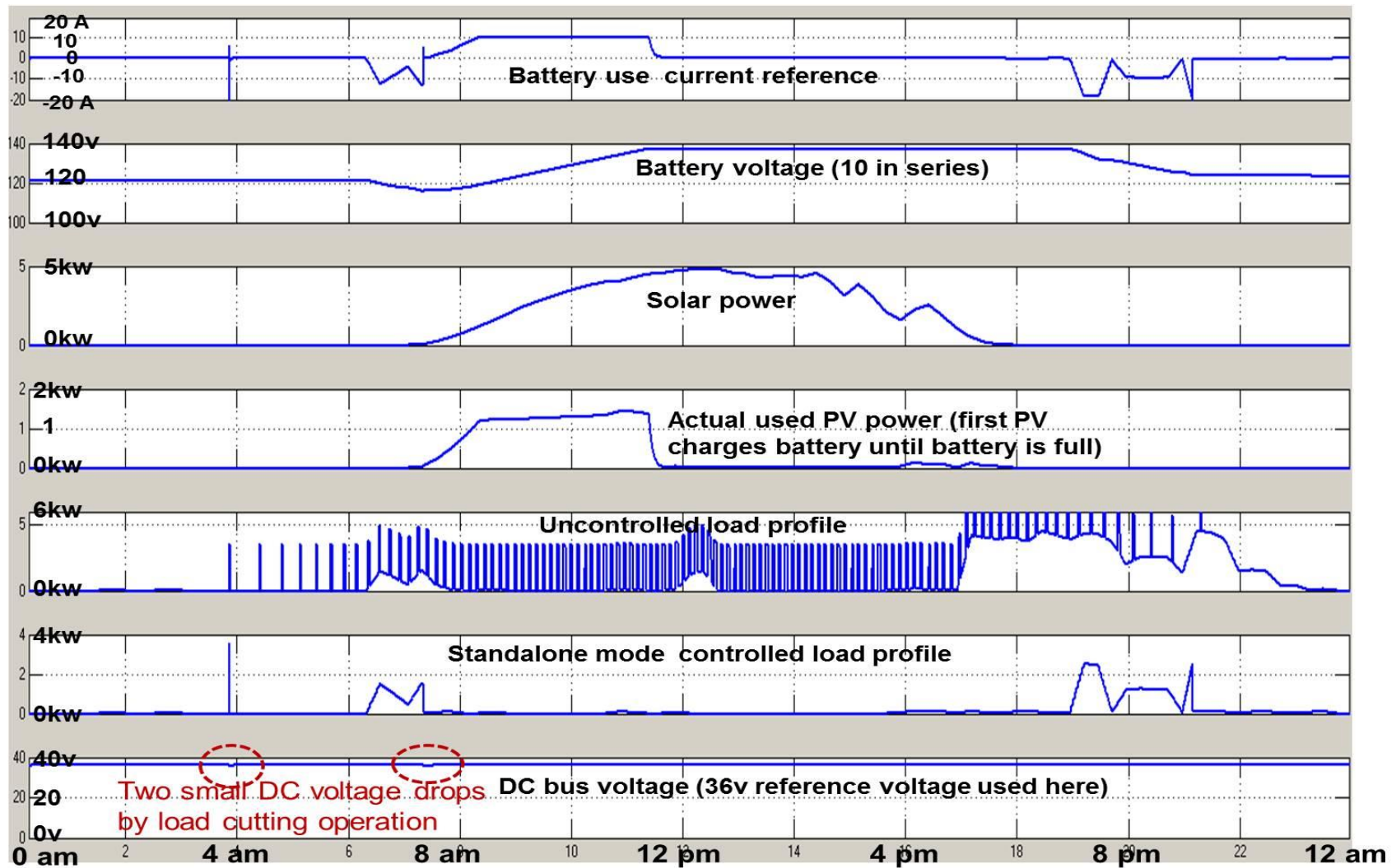


Figure 4.10 Standalone mode battery current & voltage, solar power & load power, DC bus voltage plot

absorption ability, the solar power is regulated to be shunt, and we can see this from the actual PV usage plot “Actual used PV power” in Figure 4.10. And later at around 19pm, solar power again is in outage, and the fully recharged battery supply the total loads.

4.5 CONCLUSION

Both optima and rule-based methods are available to realize SGPN system yet give users certain degree of electric cost saving. And comparing to a rule-based method making decision upon present information, optima model method synthesizes much larger size of system’s present and predictive information to provide a system control schedule input. So it can make more cost savings and more reliability if all the information predicted sufficiently accurate. However, this also inevitably leads to more complexity and more cost on the controller hardware and more dependence on peripheral algorithms software, such as power predictive algorithms. On the other hand, rule-based algorithm can be easily implemented to fulfill the control requirement in three different operation modes, such as standalone mode, in which optima method still can’t be applied for its less accuracy and slower calculation speed. So depending on whether there is standalone mode operation requirement and whether it is limited hardware or development period required application scenario, we can choose rule-based method or optima based method. In the future, as the development of more advanced peripheral algorithms and computing hardware, we can expect a more prospective application for the optima model method in smart grid and maybe other areas.

REFERENCES

- [1] C. Michael Hogan. "Fossil fuel." Internet: www.eoearth.org/view/article/152839/ , May. 26, 2013 [Sept. 1, 2013].
- [2] U.S. Department of Energy. "Smart Grid / Department of Energy." Internet: energy.gov/oe/services/technology-development/smart-grid [Sept. 1, 2013].
- [3] GridPoint Inc. "Gridpoint Energy Management Systems." Internet: www.gridpoint.com/ems-overview/ems-overview [Sept. 3, 2013].
- [4] D. J. Livengood. "The Energy Box: Comparing Locally Automated Control Strategies of Residential Electricity Consumption under Uncertainty." PhD dissertation, Massachusetts Institute of Technology, US, 2011.
- [5] P. Mahat, Z. Chen, B. Bak-Jensen. "Review of islanding detection methods for distributed generation," in *Electric Utility Deregulation and Restructuring and Power Technologies*, 2008, pp. 2743-2748.
- [6] U.S. Department of Energy. (2012, March). *Buildings Energy Data Book*. [Online]. Available: buildingsdatabook.eren.doe.gov/docs/xls_pdf/2.1.6.pdf [Sept. 3, 2013].
- [7] H. Allcott . "Real-time Pricing and Electricity Markets." Internet: economics.stanford.edu/files/Allcott3_13.pdf, Feb. 5, 2009 [Sept. 3, 2013].
- [8] B. Stalling, R. Motte, T. Clemmer, H. A. Mantooth, R. Dougal. "Design and Evaluation of a Universal Power Router for Residential Applications," in *Energy Conversion Congress and Exposition*, 2012, pp. 587-594.
- [9] D. Shanxu, C. Changsong and C. Tao. "Forecasting Power Output for Grid-connected Photovoltaic Power System without using Solar Radiation Measurement," in *IEEE International Symposium on Power Electronics for Distributed Generation Systems*, 2010, pp. 773-777.
- [10] J. Tsutsumi, T. Katayama, A. Ishii, P. He, T. Hayashi. "Investigation and numerical simulation of the wind effects on thermal comfort in a house." *Journal of Wind Engineering and Industrial Aerodynamics*, vol. 60, pp. 267-280, Apr. 1996.
- [11] U.S. Department of Energy by the National Renewable Energy Laboratory (NREL). "Battery Power for Your Residential Solar Electric System." Internet: www1.eere.energy.gov/solar/pdfs/31689.pdf, Oct. 2002 [Sept. 3, 2013].

- [12] M. Ceraolo. “New Dynamical Models of Lead–Acid Batteries.” *IEEE Transactions on Power Systems*, vol. 15, no. 4, pp. 1184-1190, Nov. 2000.
- [13] D. Linden, T.B. Reddy. “LEAD-ACID BATTERIES,” in *Handbook of batteries*, 3rd ed., Alvin J. Salkind, Anthony G. Cannone, and Forrest A. Trumbure, Ed. New York, NY: McGraw Hill, 2001, p. 76.
- [14] S. Bhattacharya, L. Anderson, S. Teleke, M. E. Baran, A. Q. Huang. “Control Strategies for Battery Energy Storage for Wind Farm Dispatching.” *IEEE Transactions On Energy Conversion*, vol. 24, no. 3, pp. 725-732, Sept. 2009.
- [15] S. J. Hou , Y. Onishi, S. Minami, H. Ikeda, M. Sugawara, A. Kozawa. “Charging and Discharging Method of Lead Acid Batteries Based on Internal Voltage Control.” *Journal of Asian Electric Vehicles*, vol.3 no.1, pp.733-737, June 2005.
- [16] S. Duryea, S. Islam, W. Lawrance, “A battery management system for stand alone photovoltaic energy systems.” *Industry Applications Conference, 1999. Thirty-Fourth IAS Annual Meeting. Conference Record of the 1999 IEEE*, vol.4, pp.2649-2654, 1999.
- [17] OPTIMA Batteries Inc. Internet: www.batteryweb.com/spec-sheet/optima/75-25-8022-091-red-top.pdf, Dec. 2008 [Oct. 15, 2013].
- [18] D. Linden, T.B. Reddy. “LEAD-ACID BATTERIES,” in *Handbook of batteries*, 3rd ed., Alvin J. Salkind, Anthony G. Cannone, and Forrest A. Trumbure, Ed. New York, NY: McGraw Hill, 2001, p. 50.
- [19] H. Bindner , T. Cronin , P. Lundsager , J. F. Manwell , U. Abdulwahid and L. Baring-Gould. “Lifetime modelling of lead acid batteries.” Internet: orbit.dtu.dk/fedora/objects/orbit:88309/datastreams/file_7710966/content, Apr. 2005 [Oct, 15, 2013].
- [20] S. Bacha, Y. Riffonneau. “Optimal Power Flow Management for Grid Connected PV Systems With Batteries.” *IEEE Transactions on Sustainable Energy*, vol. 2, no. 3, pp. 309-320, July 2011.
- [21] Xantrex International. “Temperature Compensated Charging of Lead Acid Batteries.” Internet: www.tekrispower.com/pdfs/xantrex/Batteries%20-%20Temperature%20Compensated%20Charging.pdf, May 1999 [Oct. 18, 2013].
- [22] S. Teleke, M. E. Baran, S. Bhattacharya, A. Q. Huang. “Rule-Based Control of Battery Energy Storage for Dispatching Intermittent Renewable Sources.” *IEEE Transactions On Sustainable Energy*, vol. 1, no. 3, pp. 117-124, Oct. 2010.
- [23] B. Lu, M. Shahidehpour. “Short-Term Scheduling of Battery in a Grid-Connected PV/Battery System.” *IEEE Transactions On Power Systems*, vol. 20, no. 2, pp.1053-1061, May 2005.

- [24] L. V. Pérez, G. R. Bossio¹, D. Moitre, G. O. García¹. “Optimization of power management in an hybrid electric vehicle using dynamic programming.” *Mathematics and Computers in Simulation*, vol. 73, issues 1–4, pp. 244–254, Nov. 2006.
- [25] Wikipedia. “HVAC.” Internet: en.wikipedia.org/wiki/HVAC, Oct. 8, 2013 [Oct. 21, 2013].
- [26] The MathWorks, Inc. “sldemo_househeat model.” Internet: www.mathworks.com/products/simulink/model-examples.html?file=/products/demos/shipping/simulink/sldemo_househeat.html, Oct. 8, 2013 [Oct. 21, 2013].
- [27] N. Femia, G. Petrone, G. Spagnuolo, Massimo Vitelli. “Optimization of Perturb and Observe Maximum Power Point Tracking Method.” *IEEE Transactions On Power Electronics*, vol. 20, no. 4, pp.963-973, July 2005.
- [28] IEEE. “IEEE Guide for Control Architecture for High Power Electronics (1 MW and Greater) Used in Electric Power Transmission and Distribution Systems.” *IEEE Std 1676-2010*, pp.1-47, Feb. 11, 2011.

APPENDIX A

SGPN HARDWARE STRUCTURE

A.1 SUBSYSTEM COMPONENTS

A.1.1 ON-SITE ENERGY SOURCE

On-site energy source enables the SGPN system's electric self-supply ability, which would give benefits to electric providers and consumers in two ways. One is SGPN would use on-site generated power to supply home loads and reduce grid power burden in automatic response mode and load curtailment mode. The other is in standalone mode (grid is disconnected from the system for electric shortage) the system can guarantee the basic loads working for a considerable period.

The choice of on-site energy source could be varying from solar energy source (photovoltaic panel), wind energy source (wind turbine) to any other available sources. This empowers the system to incorporate renewable energy and contribute to reduction of green-house gas emission. And in our system, solar energy is adopted.

A.1.2 OFF-SITE ENERGY SOURCE

Off-site energy source here refers to the traditional grid source. It still exists in the system to provide sufficient supply ability and stabilize the power consumption since solar energy, which is directly influenced by weather condition and daytime length, has limited capability to supply total home loads all the time by itself and obviously the power produced by these sources has uneven manner daily.

A.1.3 ENERGY STORAGE SYSTEM

Energy storage system is necessary for our system because it can realize cost saving for customers by energy usage shift, which means putting electricity into storage system at low electric price period and feed energy back into loads at high price period. Besides, in standalone mode, it is essential to increase system's supply ability and maintain power stability, since in this mode there are only two energy sources, on-site energy source mentioned above and energy storage system.

Since it is mentioned in Chapter 3, lead-acid battery is best for residential power storage system, we adopt lead-acid batteries as energy storage unit in our system.

A.1.4 LOADS SYSTEM

Loads are the group of applications homeowners most concern. In a typical house electric usage scenario, there are high power loads, such as air-conditioning, water heater and low power loads like microwave, refrigerator and television.

A.2 INTERMEDIATE CONNECTION COMPONENTS

A.2.1 AC AND DC BUSES

The reasons for intermediate connection parts are the electrical configuration difference. Off-site energy source uses AC (alternating current) input while PV panel provides DC (direct current) input. This physical configuration difference decides that there should be two buses, one AC bus with off-site energy source and all AC devices connected and one DC bus with PV panel, lead-acid battery system and all DC devices connected. In our system, AC bus is 60Hz, 240V RMS and DC bus is set to 36V (36V, 48V or other value dependent on desired PV and battery configuration) according to present PV and battery capacity as a 2kw low power prototype SGPN model.

A.2.2 INVERTER AND RECTIFIER

There should be a bridge between AC side and DC side, which gives the system bi-directional power flow capability. This bridge is called inverter / rectifier, and it functions as inverter when converting DC power into AC power, and functions as rectifier when converting AC power into DC power. In our system, the power flow direction is controlled by reference current positive and negative sign to represent DC to AC and AC to DC respectively and power flow amount is controlled by reference current absolute value.

A.2.3 PV CONVERTER

PV converter is a boost type DC/DC converter in our system. The reason for this choice is that buck type converter requires additional input capacitor to work in continuous input current mode and buck/boost converter is not necessary for our system. This buck type capacitor is generally an electrolyte capacitor for a high voltage input and thus is not suitable for high frequency application. Besides, guaranteeing the reliability of input capacitor needs additional hardware and software and therefore we use boost type to reduce total system cost.

PV boost converter is used to raise solar generator input voltage to the desired DC bus voltage and control the amount of solar electric input power. This PV power control has two cases: MPPT mode and non-MPPT mode, where MPPT means maximum power point tracking. In most system working conditions PV converter is kept running in MPPT mode, except for an extreme condition in standalone mode, if PV input power over the total amount of load consumption and battery system fully charged, PV converter will be disabled to automatically follow load.

The necessity of MPPT is that the maximum output power of a PV panel keeps changing during one day, due to varying real-time insolation and all sorts of fluctuating factors related to influence solar input power, such as cloudiness, temperature, humidity and PV load coupling level. There should be an algorithm to adjust the total coupling load by changing PV boost converter duty cycle to maximize output power and the usage efficiency of PV generator.

There have been a lot of different methods to implement MPPT, but a widely used and simple one is called “Perturb & Observe” (P&O) method [27]. This method applies a positive or negative small increment (Perturb) on duty cycle and keeps monitoring (Observe) the changing output power, product of PV output voltage and current. If the change is positive, the duty cycle is further perturbed in that direction, otherwise it is perturbed in the opposite direction. And in this thesis we only discuss which MPPT algorithm is adopted instead of developing a new MPPT algorithm.

A.2.4 BATTERY CONVERTER

Battery is a DC voltage device and is connected to DC bus through DC/DC converter. In our system, battery charging and discharging are both required, so we use buck/boost converter to realize this bidirectional power flow control. Battery is charged or discharged according to battery current reference determined by high level control system. And high level control algorithm needs state of charge (SOC) information to regulate battery use in a safe range. The lead acid battery modeling and control issues are discussed in Chapter 3 in detail.

A.2.5 LOADS SWITCHES GROUP

Load switches group is connected between AC bus, DC bus and responding loads. It is used to turn off and turn on loads designated by SGPN load management algorithm, which is discussed in Chapter 3.

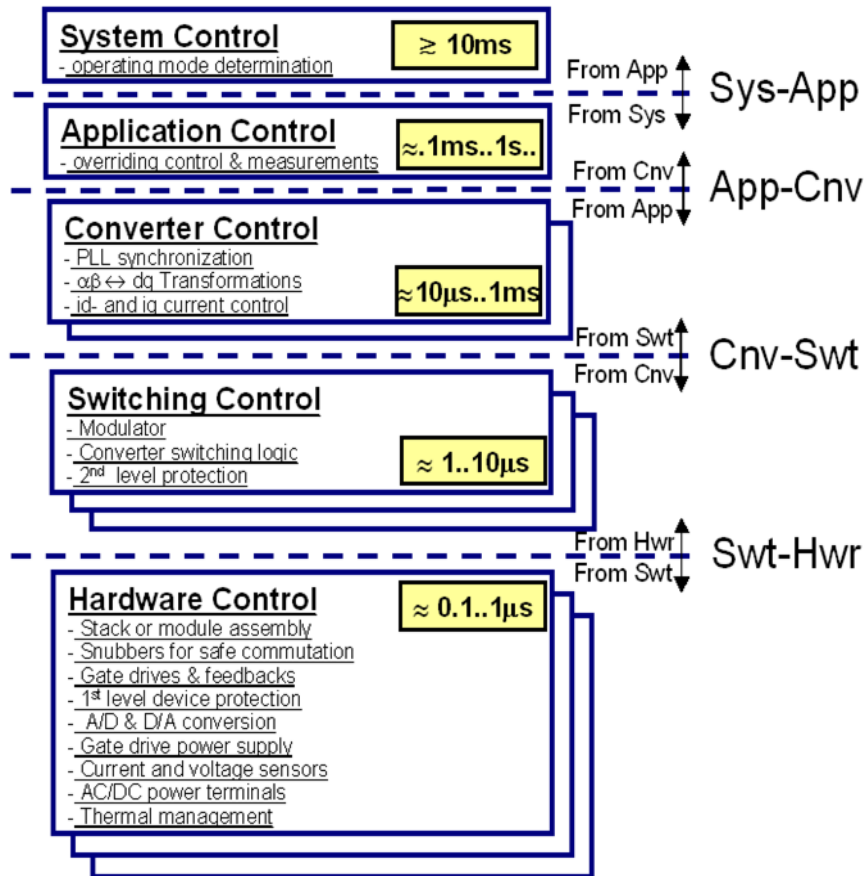


Figure A.1 SGPN Control 5-layer Hierarchy Architecture

A.3 HIGH LEVEL AND LOW LEVEL CONTROL HIERARCHY

The SGPN control hierarchy architecture is based on IEEE 1676-2010, Guide for Control Architecture for High Power Electronics (1 MW and Greater) Used in Electric Power Transmission and Distribution Systems [28]. Our present system is 2 KW prototype model farther below 1 MW level, but this architecture is still suitable for high

level control and low level system implementation. This architecture defines each layer with different operating speed requirements and functions to allow a robust control system.

This diagram Figure A.1 is similar to a cross-section of system's operation, which shows how an operation is executed from top command to bottom hardware components' action through five different functional layers.